RESEARCH ARTICLE

Cold-seep fossil macrofaunal assemblages from Vestnesa Ridge, eastern Fram Strait, during the past 45 000 years

Elsebeth Thomsen[1], Tine Lander Rasmussen[2], Kamila Sztybor[3], Nils-Martin Hanken[45], Ole Secher Tendal[6] & Alfred Uchman[7]

[1]The Arctic University Museum of Norway, UiT—The Arctic University of Norway, Tromsø, Norway;
[2]Centre for Arctic Gas Hydrate, Environment and Climate, Department of Geosciences, UiT—The Arctic University of Norway, Tromsø, Norway;
[3]Akvaplan-niva AS, Fram Centre, Tromsø, Norway;
[4]Department of Geosciences, UiT—The Arctic University of Norway, Tromsø, Norway;
[5]Department of Geosciences, University of Oslo, Oslo, Norway;
[6]Natural History Museum of Denmark, Zoological Museum, Copenhagen Ø, Denmark;
[7]Jagiellonian University, Institute of Geological Sciences, Kraków, Poland

Abstract

Four cores from 1200 m water depth from Vestnesa Ridge on the western Svalbard margin in the eastern Fram Strait were studied for their content of fossil macrofaunas. Three of the cores were collected from a pockmark with active methane seepage, and one core (control core) was taken just outside the seepage area for comparison. Together the cores cover the last 45 000 years (mid-late Weichselian glacial, the deglaciation and the Holocene). The records show a range of influence of methane from no seepage (control core) and, although variable through time, from moderate seepage, to strong and very strong seepage. All cores have been analysed for the macrofossils >1 mm, trace fossils, planktic foraminifera, stable isotopes, geochemistry and sedimentology. The main purpose of the study is to improve our knowledge of the fossil macrofauna and past environmental changes related to the impact of methane emissions in the area. The core recovered outside the pockmark contained no fossil macrofaunas, while cores from inside the pockmark contained chemosymbiotic bivalves, and in some cases a rich macrofauna. The faunal relationships with the sedimentary environments confirm a close connection between the macrofauna and the variability in influence of cold seepage, particularly seen in the occurrence of chemosymbiotic bivalves *Archivesica arctica, Isorropodon nyeggaensis*, potentially chemosymbiotic bivalve *Rhacothyas kolgae*, polychaetes and an associated rich fauna of small epifaunal gastropods, showing that Arctic seeps were oases for macrofaunas in the past as they are today.

To access the supplementary material, please visit the article landing page

Keywords

Methane release; macrofossils; trace fossils; foraminifera; mid-late Weichselian glacial to Holocene; Svalbard margin

Correspondence

Elsebeth Thomsen, The Arctic University Museum of Norway, UiT—The Arctic University of Norway, NO-9037 Tromsø, Norway. E-mail: elsebeth.thomsen@uit.no

Abbreviations

AMS: accelerator mass spectrometry
H1: Heinrich Stadial 1
MIS: Marine Isotope Stage

Introduction

The Vestnesa Ridge gas hydrate system has been the subject of extensive geophysical studies (Eiken & Hinz 1993; Vogt et al. 1994; Hustoft, Bünz et al. 2009; Petersen et al. 2010; Bünz et al. 2012; Plaza-Faverola et al. 2015). These studies, in addition to constraining the major stratigraphic sequences, have allowed pockmarks, gas migration pathways and gas hydrate distribution in the area to be mapped. Vestnesa Ridge is close to the spreading zones of the Knipovitch and Molloy mid-ocean ridges and subject to intense faulting. The tectonic stress at Vestnesa Ridge most likely exerts the major control of change in seepage intensity (Plaza-Faverola et al. 2015; Plaza-Faverola & Keiding 2019). Smaller scale factors superimposed on the tectonic forcing are, for example, sea-level change on a glacial–interglacial scale (e.g., Teichert et al. 2003; Cook et al. 2011), increased seismic activity from ice retreats and glacial rebounds (e.g., Wallmann et al. 2018) and rapid sediment loading during deglaciations (e.g., Hustoft et al. 2009; Hill et al. 2012).

Limited work has been done so far toward improving our knowledge of the short-term episodic changes in the upward methane flux at Vestnesa Ridge and the impact on micro- and macrofaunas and the sedimentary environments. Fossil chemosynthetic macrofaunal assemblages give direct evidence of the presence of hydrogen sulphide-rich fluids in near-surface sediments (e.g., Sahling et al. 2003; Lartaud

Citation: *Polar Research* 2019, *38*, 3310, http://dx.doi.org/10.33265/polar.v38.3310

et al. 2010; Decker & Olu 2012; Decker et al. 2012; Marcon et al. 2014). The hydrogen sulphide is a product of anaerobic methane oxidation mediated by a microbial consortium of methanogenic archaea and sulphate-reducing bacteria (Boetius et al. 2000). It serves as an energy source for filamentous sulphur bacteria, bivalves and tubeworms hosting chemoautotrophic bacteria in their tissues (Paull et al. 1984; Brooks et al. 1987; Macdonald et al. 1989; Levin 2005). In the oligotrophic environment of the deep sea, restricted by organic flux from the surface to the bottom, the microbial process of anaerobic methane oxidation serves as the base of a food chain and often promotes enhanced benthic productivity compared to areas outside methane seeps (Paull et al. 1984; Brooks et al. 1987; Thomsen 1987; Sahling et al. 2003; Åström et al. 2016; Åström et al. 2018). The close association between seabed fluid flow and "anomalous" rich benthic communities has been described from many different locations worldwide (Hovland & Thomsen 1989; MacDonald et al. 1989; Olu et al. 1997; Levin et al. 2003; Hovland 2008). In addition to endemic seep species, the high concentration of chemoautotrophic-derived organic matter attracts other heterotrophic organisms, including megafaunas (e.g., Sahling et al. 2003; Levin 2005).

In this study, we focus on the occurrence of macrofaunal assemblages (fossils >1 mm and trace fossils) with the purpose of investigating the relationship between the assemblages and the sedimentary environments and the impact of seeping of methane on the faunas and environment in four gravity cores from Vestnesa Ridge, eastern Fram Strait. The investigated material is derived from three cores from a pockmark and one core from outside, which have been analysed for the presence or absence of macrofaunas and species distribution through time. An earlier multiproxy study of these four cores comprising lithological changes, oxygen and carbon isotopes, foraminiferal fauna distribution patterns, the presence or absence of authigenic carbonates, magnetic susceptibility, x-ray fluorescence data, % total organic carbon, % $CaCO_3$ and AMS ^{14}C datings showed that the cores represent a range of increasing intensity of seepage from none (control site outside pockmark), through moderate and strong, to very strong seepage (Sztybor & Rasmussen 2017a). The methane seepage was also highly variable through time. Pore water analyses of new cores taken in 2016 and 2017 at the same positions as these four cores, or close to them, show that the depth of the sulphate–methane transition zone ranges from >4 m (non-seep site), through 1.2 m at the site of moderate seepage and 40 cm at the site with strong seepage, to 5–20 cm close to the site of strongest seepage (Laier et al. 2017; see also Hong et al. 2016).

For this study, the two cores from areas within the pockmark of the most intense seeping with the most severe degree of disturbance from seepage have been re-investigated for the content of planktic foraminiferal faunas and authigenic carbonate nodules, and supplemented by new AMS ^{14}C dates for stratigraphical purposes. New stable isotope analyses of the epibenthic foraminiferal species *Cibicidoides wuellerstorfi*/*Cibicides lobatulus* in the three cores from within the pockmark are compared to previously published data on the endobenthic foraminiferal species *Cassidulina neoteretis* to further our understanding of macrofaunal changes in relation to past methane seepage.

Study area

Vestnesa Ridge is a sediment drift located at the western Svalbard margin at water depths between ca. 1200 and 1300 m (Fig. 1). It was formed by bottom currents

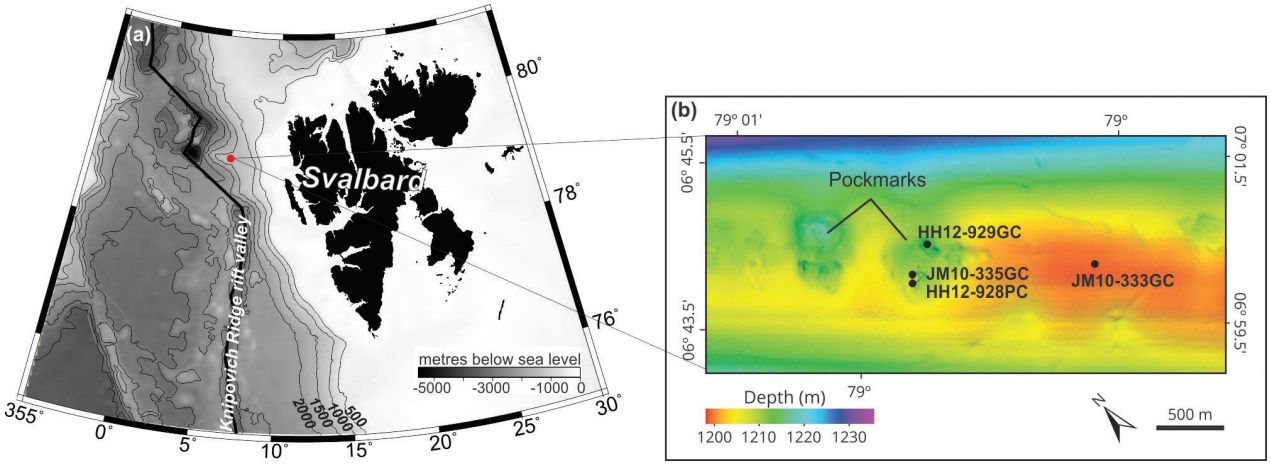

Fig. 1 Location maps. (a) Section of the Fram Strait and Svalbard showing the location of Vestnesa Ridge study area (red dot). (b) Bathymetry of the investigated area based on data from Bünz et al. (2012) showing pockmarks and location of core sites.

Citation: *Polar Research* 2019, *38*, 3310, http://dx.doi.org/10.33265/polar.v38.3310

from the late Miocene onwards (Eiken & Hinz 1993). Late Quaternary sediments consist of contourite and glaciomarine deposits (Howe et al. 2008). The crest of Vestnesa Ridge is perforated with pockmarks suggested to be generated by methane venting (Vogt et al. 1994). This was later confirmed by extensive geophysical studies (Hustoft, Bünz et al. 2009; Petersen et al. 2010; Bünz et al. 2012; Plaza-Faverola et al. 2015), which documented methane release from the pockmarks at the south-eastern part of the ridge and the presence of methane hydrates in sediment cores (Fisher et al. 2011). Acoustic flares rising from the seafloor in the area are frequently observed hydroacoustically (Hustoft, Bünz et al. 2009; Bünz et al. 2012). Tubeworms and patches with white bacterial mats (probably *Beggiatoa*), indicating areas of active gas seeping, have been observed in the pockmarks (Vinogradov 1999; Åström et al. 2018).

Vestnesa Ridge is affected by the West Spitsbergen Current, which flows northwards along western Svalbard (Schauer et al. 2004; Walczowski et al. 2005). This current consists of the relatively warm and saline Atlantic surface water (T<3–6°C and S ca. 35) derived from the North Atlantic Current and the deeper intermediate water (−0.9°C) derived from convection of surface water in the Nordic seas to cold deepwater (e.g., Hopkins 1991). The warm surface current maintains ice-free conditions in the eastern Fram Strait throughout most of the year (Aagard et al. 1987; Schauer et al. 2004; Walczowski et al. 2005).

Material and methods

Two gravity cores—JM10-333GC and JM10-335GC—were collected from a water depth of 1200 m on the Vestnesa Ridge in June 2010 during a cruise with the RV *Jan Mayen* (subsequently renamed RV *Helmer Hanssen*; Fig. 1). Core JM10-335GC was taken from inside a pockmark from within a rising gas flare observed on the echo-sounder, while core JM10-333GC was taken outside the pockmark in normal hemipelagic sediments as a control core. These two cores were previously AMS ^{14}C dated and investigated for benthic and planktic foraminiferal faunas, grain size, ice-rafted debris, % total organic carbon and % $CaCO_3$, and—for core JM10-335GC only—stable isotopes analyses were carried out on the planktic foraminiferal species *Neogloboquadrina pachyderma* and the benthic species *Cassidulina neoteretis* and *Melonis barleeanus* (Sztybor & Rasmussen 2017a, b). Two additional cores—piston core HH12-928PC and gravity core HH12-929GC—were taken in July 2012 from inside the same pockmark during a cruise with the RV *Helmer Hanssen* (Fig. 1). For these cores, stable isotope analyses of the same species as for JM10-335GC were performed.

Details of core handling have been described previously (Sztybor & Rasmussen 2017a, b). For this study, the same sample sets in 1-cm-thick slices at 5-cm intervals were used. For macrofaunas, all preserved parts of organisms (e.g., tubes from polychaetes), fossils and trace fossils from >1 mm size fractions were sorted out and identified. The trace fossils were preserved as burrows in carbonate concretions and borings in bivalves and gastropods. The generally poor preservation caused by encrustation and carbonate cementation in primary cavities of the bivalves and gastropods made it difficult to identify many of the fossils to species level.

Cores HH12-929GC and HH12-928PC were also studied for planktic foraminiferal content and carbonate concretions (nodules) were counted in the samples from core HH12-929GC. The same procedures used by Sztybor & Rasmussen (2017a, b) were followed for counts of foraminifera and ice-rafted debris. Carbonate nodules are authigenic carbonate precipitated in sediments affected by methane seepage as another "by-product" of anaerobic methane oxidation and sulphate reduction by the bacteria and archaea (Boetius et al. 2000). The precipitation of authigenic carbonate is related to high rates of methane oxidation taking place near the sediment surface (Borowski et al. 1996; Fontanier et al. 2014) and can be used as a sign of palaeo-seepage (Schneider et al. 2017). These nodules are similar to the "carbonate mud clasts" described by Fontanier et al. (2014), with sediment and foraminifera embedded. They are also referred to as "methane-induced authigenic carbonates" (MDAC) or "carbonate crusts/carbonate encrustations." In core HH12-928PC, the crusts, pavements and nodules are so abundant that they could not be quantified reliably; for this core, we present the weight percentage of particles in the >0.5 mm size fraction, which mainly consists of authigenic carbonates and only minor amounts of ice-rafted debris. No encrustations were found in cores JM10-333GC from outside the pockmark or in JM10-335GC from the pockmark.

For the three pockmark cores—JM10-335GC, HH12-928PC and HH12-929GC—new stable isotope analyses were performed on specimens of the epibenthic foraminiferal species *Cibicides lobatulus* and *Cibicidoides wuellerstorfi* (3–13 specimens). For JM10-335GC, only specimens of *C. wuellerstorfi* were analysed. In HH12-929GC, the two species were analysed separately. In HH12-928PC, the species were mixed because encrustation of most foraminifera by authigenic carbonates limited the amounts of suitable (pristine) specimens. Analyses were done at the Bjerknes Centre for Climate Change, University of Bergen, Norway, following the same procedures outlined

by Sztybor & Rasmussen (2017a). The results for both species have been corrected for isotopic disequilibrium of 0.64‰ (Shackleton 1974).

For this study, three new AMS ^{14}C dates of samples from core HH12-929GC and three from core HH12-928PC were obtained at 14Chrono Centre, Queens University Belfast, Northern Ireland (Table 1). New dates and previously published dates for all four records were calibrated (and re-calibrated, respectively) using the Calib7.04, Marine13 dataset (Table 1; Fig. 2). All ages were corrected for standard global reservoir effect -405 years inherent in the Calib programme (Stuiver & Reimer 1993; Reimer et al. 2013). The mid-point of the probability range 1σ was calculated for each calibrated age. All ages reported here are in calendar years before the present, unless otherwise specified.

Results

Lithology, stratigraphy and age models

Our findings regarding the lithology, stratigraphy and stable isotopes and our construction of the age models have been published previously (Fig. 2). For cores HH12-929GC and HH12-928PC, new data on planktic foraminiferal distribution patterns, new stable isotope analysis results and new dates are presented here, refining our earlier age models.

Control core JM10-333GC. The oldest part of the core consists of brown hemipelagic sediments with numerous clasts >2 mm (Fig. 2). Several short sequences of light brown material occur until 285 cm. Between 285 and 265 cm, there is a coarse-grained dark layer of unsorted sediments with sharp boundaries (Fig. 2). Jessen et al.

Table 1 AMS ^{14}C dates and calibrated ages.

Depth (cm)	AMS ^{14}C date[a]	Calibrated age	Lab. reference	Species	Reference[b]
Core JM5710-333GC					
20	12 920 ± 40	14 825 ± 166	Beta-4133010	Mixed BF[c]	1
137	14 475 ± 61	17 105 ± 120	UB-23419	*N. pachyderma* s	1
147	15 230 ± 61	18 025 ± 95	UB-23420	*N. pachyderma* s	1
359	37 420 ± 340	41 585 ± 281	Beta-412869	*N. pachyderma* s	1
Core JM10-335GC					
20	9300 ± 38	10 155 ± 39	UB-18137	*N. pachyderma* s	1
56	10 830 ± 43	12 345 ± 118	UB-23417	*N. pachyderma* s	1
57	10 820 ± 43	12 330 ± 121	UB-23418	*N. pachyderma* s and mixed BF[c]	1
75	11 830 ± 44	13 300 ± 55	UB-18138	*N. pachyderma* s	1
278	15 485 ± 73	18 335 ± 113	UB-23197	*N. pachyderma* s	1
278	15 285 ± 56	18 080 ± 98	UB-18142	*N. pachyderma* s/ and bivalve	1
290	16 830 ± 71	19 815 ± 123	UB-18139	*N. pachyderma* s	1
369	19 325 ± 77	22 780 ± 130	UB-18140	*N. pachyderma* s	1
460	27 130 ± 150	30 920 ± 113	UB-18141	*N. pachyderma* s	1
Core HH12-929GC					
5	3899 ± 36	3875 ± 55	UB-23198	*N. pachyderma* s	1
80	7219 ± 38	7678 ± 47	UB-23199	*N. pachyderma* s	1
106–109	17 795 ± 89	20 980 ± 148	UB-37798	Vesicomyid	2
140	18 010 ± 101	21 280 ± 173	UB-23200	*N. pachyderma* s	1
141	23 705 ± 176	27 540 ± 131	UB-23201	Vesicomyid	1
175.5	24 575 ± 129	28 200 ± 181	UB-37356	Vesicomyid	2
250	44 045 ± 2219	47 070 ± 1883	UB-23202	*N. pachyderma* s	1
271.5	30 515 ± 264	33 905 ± 486	UB-37357	Vesicomyid	2
311	42 175 ± 1709	45 100 ± 1550	UB-23203	*N. pachyderma* s	1
Core HH12-928PC					
1	14 550 ± 70	17 220 ± 129	UB-27838	Bivalve	1
2	22 345 ± 135	26 140 ± 142	UB-27839	Aragonite needles	1
3	14 120 ± 54	16 540 ± 133	UB-27840	Bivalve	1
53	15 210 ± 66	18 005 ± 97	UB-27841	Bivalve	1
117	25 245 ± 142	28 855 ± 166	UB-29091	Aragonite needles	2
117	13 410 ± 64	15 510 ± 91	UB-29107	Bivalve	2
197	14 350 ± 63	16 920 ± 132	UB-29092	Bivalve	2

[a]Conventional ages. [b]1 = Sztybor & Rasmussen (2017a); 2 = this study. [c]Benthic foraminiferal species.

Citation: *Polar Research* 2019, *38*, 3310, http://dx.doi.org/10.33265/polar.v38.3310

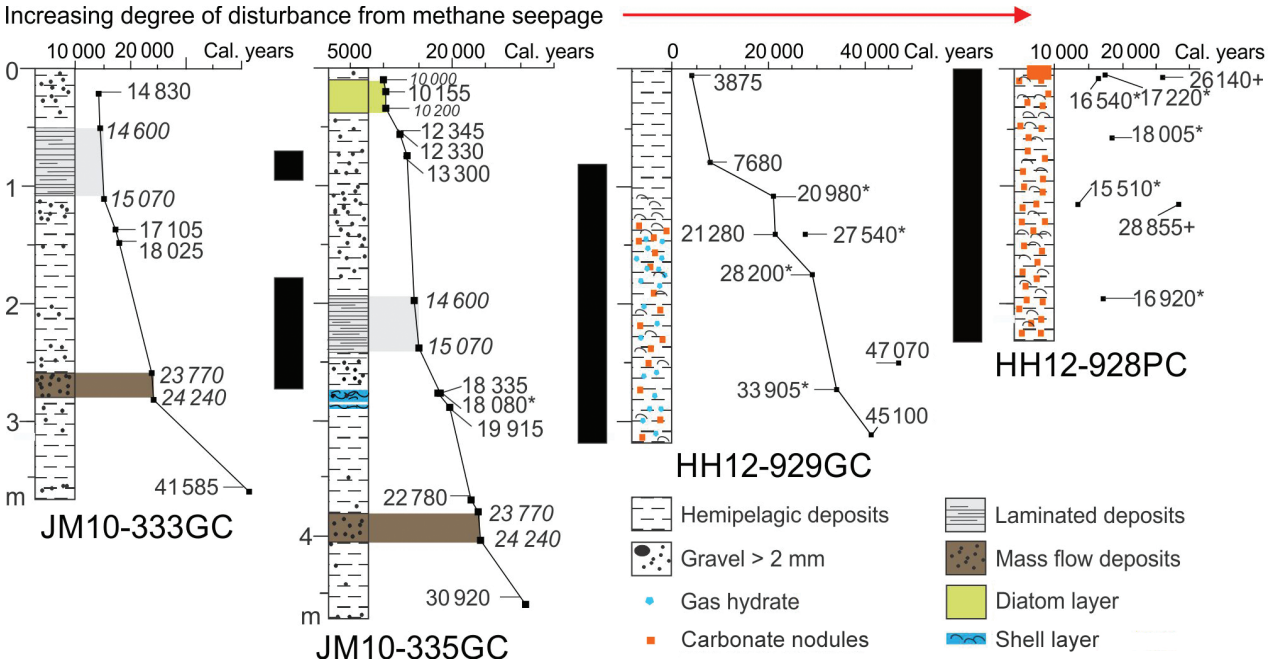

Fig. 2 Lithology of the cores with plotted AMS dates (calendar years before the present) from Sztybor & Rasmussen (2017a). Intervals of low $\delta^{13}C$ values and the presence of authigenic carbonates are indicated by black bars. Ages marked with asterisks were determined from chemosymbiotic bivalves, and the ages marked with plus signs were determined from aragonite needles. Ages in italics were derived from published ages of marker horizons from Jessen et al. (2010).

(2010) have interpreted this layer as a mass transported deposit dated to ca. 24000 years ago. Superposing is a light grey, silty clay with numerous mineral grains interpreted as ice-rafted debris, followed by a 65-cm-thick layer of fine laminated clay dating to 15070–14600 years ago (Jessen et al. 2010; Fig. 2). The upper part of the core (50–0 cm) consists of hemipelagic clayey, silty deposits with a high concentration of ice-rafted debris, probably a lag deposit. Four AMS ^{14}C dates obtained on foraminifera gave a range from 41585 to 14830 years ago, covering mid-MIS 3 to MIS 2 (Sztybor & Rasmussen 2017a; Fig. 2; Table 1).

Pockmark core JM10-335GC. Although this core was taken from a pockmark, it has an undisturbed lithology and displays the same well-known marker layers as the control core (Fig. 2). Similar to the control core, the bottom of this core penetrated through light hemipelagic sediments with several larger clasts. Between 405 and 380 cm, there is a dark brown, coarse-grained mass transported sediment layer. Further, the core consists of light grey hemipelagic sediments with two distinct layers of bivalve shells between ca. 279 and 270 cm and between 283 and 282 cm (Figs. 2, 3). Darker sediments with a high proportion of ice-rafted debris are above the shell layer and are followed by a 40-cm sequence of laminated fine clay (240–200 cm) similar to that in core JM10-333GC (Fig. 2). The remaining part of the core (200–0 cm) consists of hemipelagic deposits with decreasing amounts of ice-rafted debris and includes a layer of fine-grained, dark mud with abundant large diatoms (>63 µm). The core is characterized by a strong H_2S odour in the interval 400–0 cm and numerous gas bubbles in the sediment between 370 and 280 cm.

This core has the most complete sequence of the three cores recovered from the pockmark. Nine AMS ^{14}C dates ranging from 30920 to 10155 years ago are based on foraminifera (eight dates) and one, ca. 18080 years ago, on a shell of the vesicomyid bivalve *Archivesica arctica* (Figs. 2, 3; Table 1). The core covers upper MIS 3 to lower MIS 1 (early Holocene; Sztybor & Rasmussen 2017a).

Pockmark core HH12-929GC. The core contained gas hydrates in the lower part that were discovered when the core was cut into sections immediately after core retrieval. The hydrates occurred from the bottom to 145 cm core depth (Fig. 2). Strong H_2S odour occurred from 178 to 0 cm. A dark grey hemipelagic sediment with varying concentrations of authigenic carbonate nodules is present from the bottom to 130 cm. A layer of light grey clayey sediments with a maximum concentration of authigenic carbonate nodules occurs between 130 and 110 cm (Figs. 2, 4). The upper part of the core (ca. 100–0 cm) consists of dark homogeneous clayey silt and is devoid of carbonate nodules.

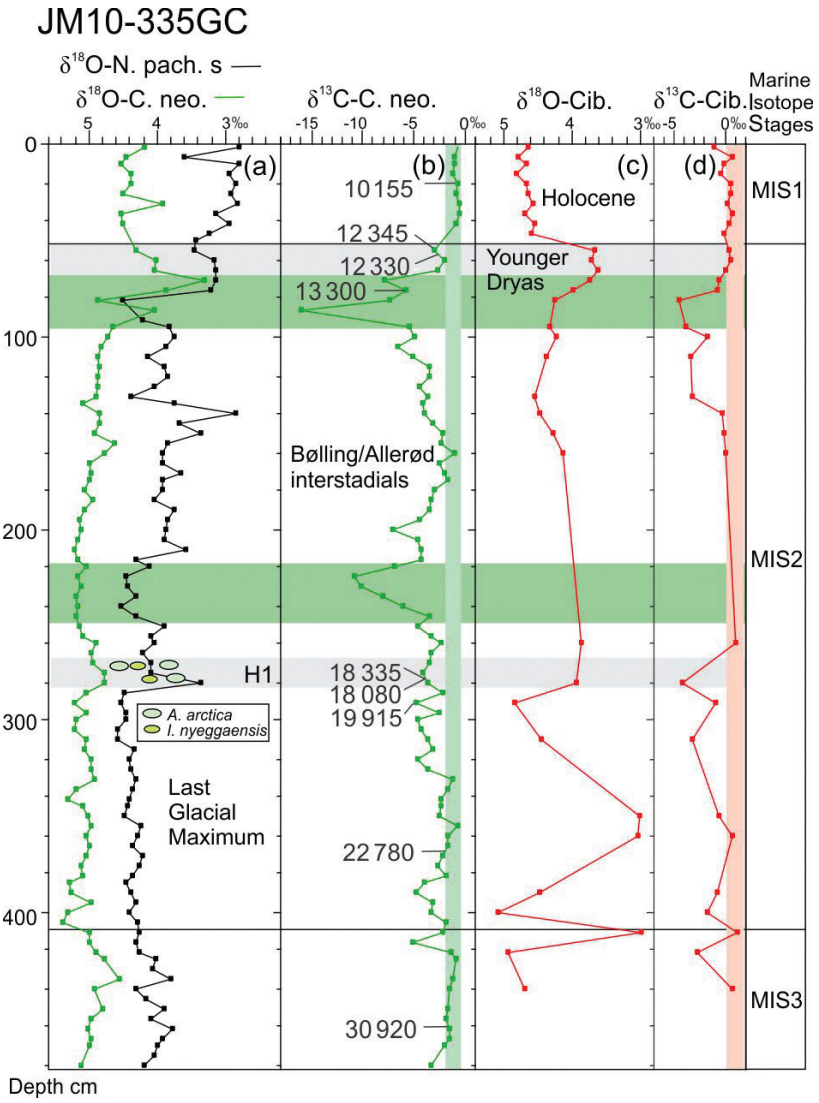

Fig. 3 Isotope data from pockmark core JM10-335GC. (a) Published planktic (*N. pachyderma* s) and benthic (*Cassidulina neoteretis*) $\delta^{18}O$ records (Sztybor & Rasmussen 2017a). (b) Published $\delta^{13}C$ record of *C. neoteretis*. (c) $\delta^{18}O$ record of *Cibicidoides wuellerstorfi*. (d) $\delta^{13}C$ record of *C. wuellerstorfi*. MISs are shown in right column. Calibrated dates are marked in (b), stratigraphy in (a) and (b). Vertical pale green and orange bars mark the range of glacial–Holocene $\delta^{13}C$ values in *C. neoteretis* (from Wollenburg et al. 2001) and *C. lobatulus*/*C. wuellerstorfi* (from Duplessy et al. 1988), respectively. Horizontal green bars mark events of lowest $\delta^{13}C$ values.

Because of disturbance of the deeper part of this core by the gas hydrate dissociation, the stratigraphy was considered uncertain (Sztybor & Rasmussen 2017a). However, with the new radiocarbon dates (Fig. 2; Table 1), it becomes clear that the two dates of 27 540 and 47 070 years ago are too old and that the lower part of the core is younger than the previous age model suggested. Radiocarbon ages instead range from 45 100 to 3875 years, ignoring the two outlier dates. It also appears that the core probably contains a hiatus around 106 cm downcore (Fig. 4). The upper 106 cm belong to the Holocene, as indicated by the low relative abundance of the polar planktic foraminiferal species *N. pachyderma* and low $\delta^{18}O$ values in *N. pachyderma*, *C. neoteretis* and *C. lobatulus*/*C. wuellerstorfi* (Fig. 4). The dates of 20 980 years ago at 107.5 cm and 21 280 years ago at 140 cm downcore together with maximum values in $\delta^{18}O$ values in both *N. pachyderma* and the benthic species indicate that this interval belongs to the Last Glacial Maximum, which took place 24 000–19 000 years ago (Lisiecki & Raymo 2005; Fig. 4). Extrapolating from the two Holocene dates (acknowledging that sedimentation rates may not have been constant for

Citation: *Polar Research* 2019, *38*, 3310, http://dx.doi.org/10.33265/polar.v38.3310

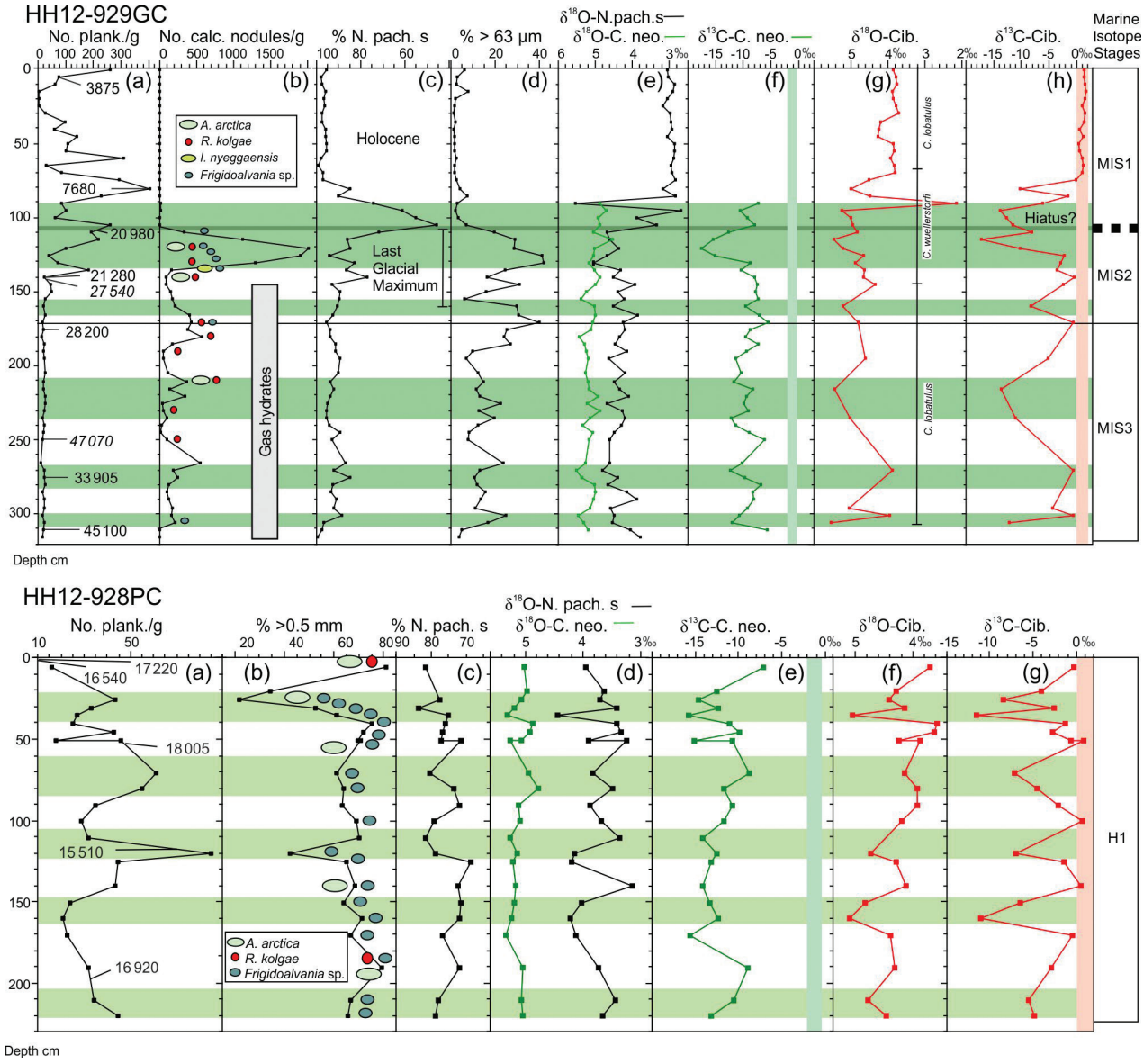

Fig. 4 (Upper panel a–h) Foraminiferal, grain size and isotope data from pockmark core HH12-929GC. (a) Concentration of planktic foraminifera in number per gram dry weight sediment with calibrated AMS ^{14}C dates indicated (discarded dates are in italics). (b) Concentration of authigenic calcareous nodules in number per gram dry weight sediment. Presence of chemosymbiotic bivalve species and of the most common gastropod *Frigidoalvania* sp. is indicated. (c) Percentage distribution of the polar planktic foraminiferal species *Neogloboquadrina pachyderma* s. (d) Weight percentage of grains >63µm. (e) Published planktic (*N. pachyderma* s) and benthic (*Cassidulina neoteretis*) δ^{18}O records (Sztybor & Rasmussen 2017a). (f) Published δ^{13}C record of *C. neoteretis*. (g) δ^{18}O record of *Cibicides lobatulus*/*Cibicidoides wuellerstorfi* (intervals of each species indicated to the right). (h) δ^{13}C record of *C. lobatulus*/*C. wuellerstorfi*. MISs are shown in right column. Vertical and horizontal bars are explained in text to Fig. 3. Horizontal green bars mark events of lowest δ^{13}C values. (Lower panel a–g) Foraminiferal, grain size and isotope data from pockmark core HH12-928PC. Same parameters as in upper panel, except that (b) shows the weight percentage of particles >0.5 mm. Vertical and horizontal bars are explained in the caption of Fig. 3. Horizontal light green bars mark events of lowest δ^{13}C values.

this long time interval in the Holocene), we calculate an age of 9000 years right above the hiatus (106 cm), indicating that the interval from ca. 21 000 to ca. 9000 years ago, comprising the late Last Glacial Maximum, the deglaciation and early Holocene, is missing. In addition, the part between 106 cm and 90 cm may be disturbed as benthic δ^{18}O values in *C. neoteretis* and *C. wuellerstorfi* are fairly high, indicating mixing of glacial and Holocene specimens (Fig. 4), while

values measured in the benthic foraminiferal species *M. barleeanus* (not shown) record Holocene values from 106 cm to the core top (see Sztybor & Rasmussen 2017a). The part deeper than 175 cm (older than 28 000 years) belongs to MIS 3 (see Lisiecki & Raymo 2005; Figs. 4, 5).

Pockmark core HH12-928PC. This core sampled hard carbonate crust throughout and is the most disturbed record of the three cores from the pockmark and was probably influenced by very strong methane seepage (Sztybor & Rasmussen 2017a; Fig. 2). It contains authigenic carbonates, including carbonate nodules of different sizes and shapes, with numerous heavily encrusted bivalve shells and only small proportions (<30%) of very dark grey fine-grained sediments (Fig. 4). Pieces of solid aragonitic pavement, encrusting numerous bivalves, are in the upper 10 cm of the core. All core sections were characterized by a strong H_2S odour.

Two AMS radiocarbon dates on unidentified vesicomyid bivalve shells drilled out from the carbonate crust range from 17 220 to 16 540 years ago, and one date on aragonite needles precipitated inside a shell gave an age of 26 140 years (Fig. 2; Table 1). Three new dates—two on unidentified chemosymbiotic vesicomyid shells—gave ages of 16 920 and 15 510 years, while aragonite needles gave an age of 28 855 years. Ignoring the obviously too old ages of the aragonite needles (Figs. 2, 4), the cored interval most likely correlates in age to the North Atlantic H1 that took place about 19 000 to 15 500 years ago (e.g., Bond et al. 1993). Given the many age reversals, the high proportions of authigenous carbonates, and the very low proportions of fine-grained sediments (weight percentages of residues <0.5 mm mostly only 20–30%; Fig. 4), it is also clear that the sediments are very disturbed. However, since the five dates, all performed on chemosymbiotic bivalves (see below) are in the age range of H1, we are confident that the fossil macrofaunas in core HH12-928PC mainly belong to this event (Figs. 2, 4, 5; Table 1).

Results and interpretation of macrofossils and trace fossils

Taxonomy and taxonomic and other notes regarding the macrofaunas are provided in the supplementary material.

Control core JM10-333GC. No macrofossils or trace fossils are present in this core, except for a badly preserved and therefore undeterminable gastropod from a depth of 282.5 cm. Only microfossils have been recovered (foraminifera and sponge spicules, this study). Sponge spicules are scattered throughout the core, but are abundant only in the top surface layer and in a sample from a depth of 237 cm. They are probably scattered by current transportation before final burial and can therefore not be used as conclusive evidence of an autochthonous sponge fauna at the location.

Interpretation: The gastropod was sampled from the layer (285–265 cm) of coarse-grained unsorted sediment that has been ascribed to a mass flow deposit (see above; Fig. 2) and must be considered allochthonous.

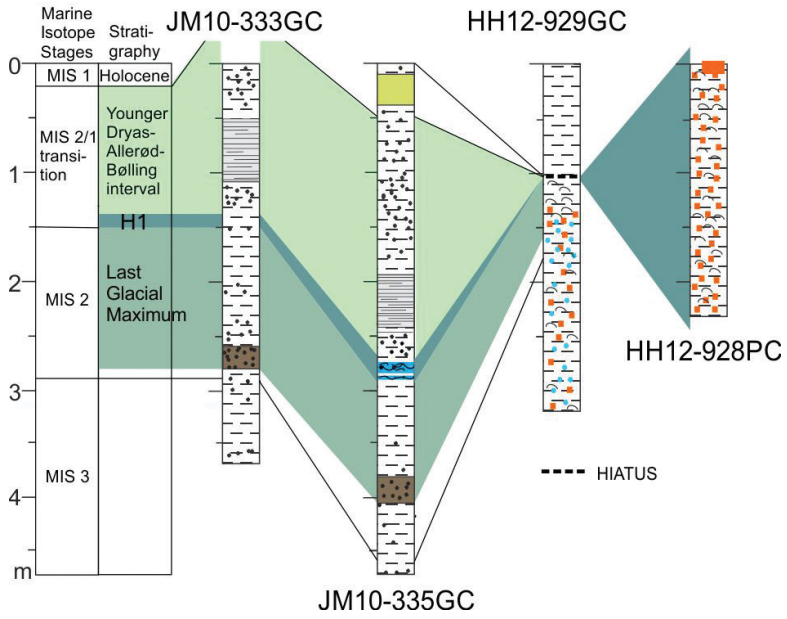

Fig. 5 Stratigraphy and correlation of the four cores. MISs and stratigraphy are shown in columns to the left. For cores JM10-333GC and JM10-335GC, the stratigraphy is from Sztybor & Rasmussen (2017a). See the lithology key in Fig. 2.

Citation: *Polar Research* 2019, *38*, 3310, http://dx.doi.org/10.33265/polar.v38.3310

The lack of a fossil macrofauna, gas hydrates and authigenic carbonates in the hemipelagic sediment/silty clay is consistent with the core's location outside the active pockmark. Clasts (ice-rafted debris) are particularly common in the upper part of the core, indicating a glaciomarine environment of the last deglaciation (Fig. 2). The lack of a macrofauna throughout the recorded time interval ca. 41 585 to 14 830 years ago confirms previously published results of diversity patterns in Arctic macrofaunas that show higher diversity (and density) in cold-seep areas than outside (Åström et al. 2016; Åström et al. 2018). Foraminiferal faunas do not show any significant differences between site JM10-333GC from outside the pockmark and site JM10-335GC from inside it (Sztybor & Rasmussen 2017b).

Core JM10-335GC from undisturbed part of the pockmark. In this core, macrofossils are confined to two layers of benthic infaunal bivalve shells, with about 30 specimens of vesicomyid species, including well-preserved whole individuals (Figs. 2, 3). There are two species—the larger *Archivesica arctica* Hansen et al., 2017 and the smaller *Isorropodon nyeggaensis* Krylova, 2011—in the material (Hansen et al. 2017) (Supplementary Notes 1, 2; Fig. 6a). A few epifaunal gastropods were also found in the bivalve shell layer. Specimens of a naticid gastropod, *Euspira* sp. and a plate of the cirriped *Verruca stroemia* (Müller, 1776) were also recovered from the shell layer.

Spicules from sponges are abundant to very abundant in the topmost 40 cm of the core. The lack of microscleres, however, made it impossible to identify the sponges to species level.

Living chemosymbiotic siboglinid polychaetes have been recovered from the seabed sediment of the core (not shown). Siboglinids are benthic sedentary organisms that live in chitinous tubes (hence the popular name tubeworms) and are anchored in soft sediment.

Interpretation: This is the record most similar to the control core regarding lithology and foraminiferal content. It appears to have been affected by methane seepage for the studied time interval, ca. 31 000–10 000 years ago, but only moderately, and the lithology has not been disturbed (Fig. 2). The $\delta^{13}C$ data (together with other parameters; see Sztybor & Rasmussen 2017a) show two periods of increased influence by seepage, correlating with the Bølling and Allerød interstadials (Fig. 3). The bivalves in the shell layer—*A. arctica* and *I. nyeggaensis*—have an age between 18 080 and 18 335 years (re-calibrated ages; Figs. 2, 3), that is, they lived during the H1 event before the start of the Bølling interstadial (see also Hansen et al. 2017; Sztybor & Rasmussen 2017a; Fig. 5). The two infaunal bivalve species—*A. arctica* and *I. nyeggaensis*—are chemosymbiotic (Krylova et al. 2001; Hansen et al. 2017).

Studies of frenulate siboglinid tubeworms (*Sclerodinum* sp. and/or *Oligobrachia* sp.) from surface sediments from the Håkan Mosby Mud Volcano and Vestnesa Ridge showed that they harbour sulphide-oxidizing endosymbionts (Pimenov et al. 2000; Sen et al. 2018). The presence of living siboglinid polychaetes confirms the present active cold-seep environment in the pockmark.

Core HH12-929GC from the deepest part of the pockmark containing gas hydrate. The lowermost part of the core between 250 and 110 cm contains a fairly diverse fossil macrofauna assemblage of bivalves and gastropods. Most abundant macrofauna are the small-sized epifaunal gastropods *Frigidoalvania* sp. and *Pseudosetia* sp. (Fig. 7) (Supplementary Note 3). The bivalves are *Rhacothyas kolgae* Åström & Oliver, 2017, *Archivesica arctica* and *Isorropodon nyeggaensis* (Figs. 4, 7; Supplementary Note 4).

Fig. 6 (a) *Archivesica arctica* from the shell layers in core JM10-335GC (TSGF 18357–18358). (b) *Rhachothyas kolgae* from core HH12-929GC.

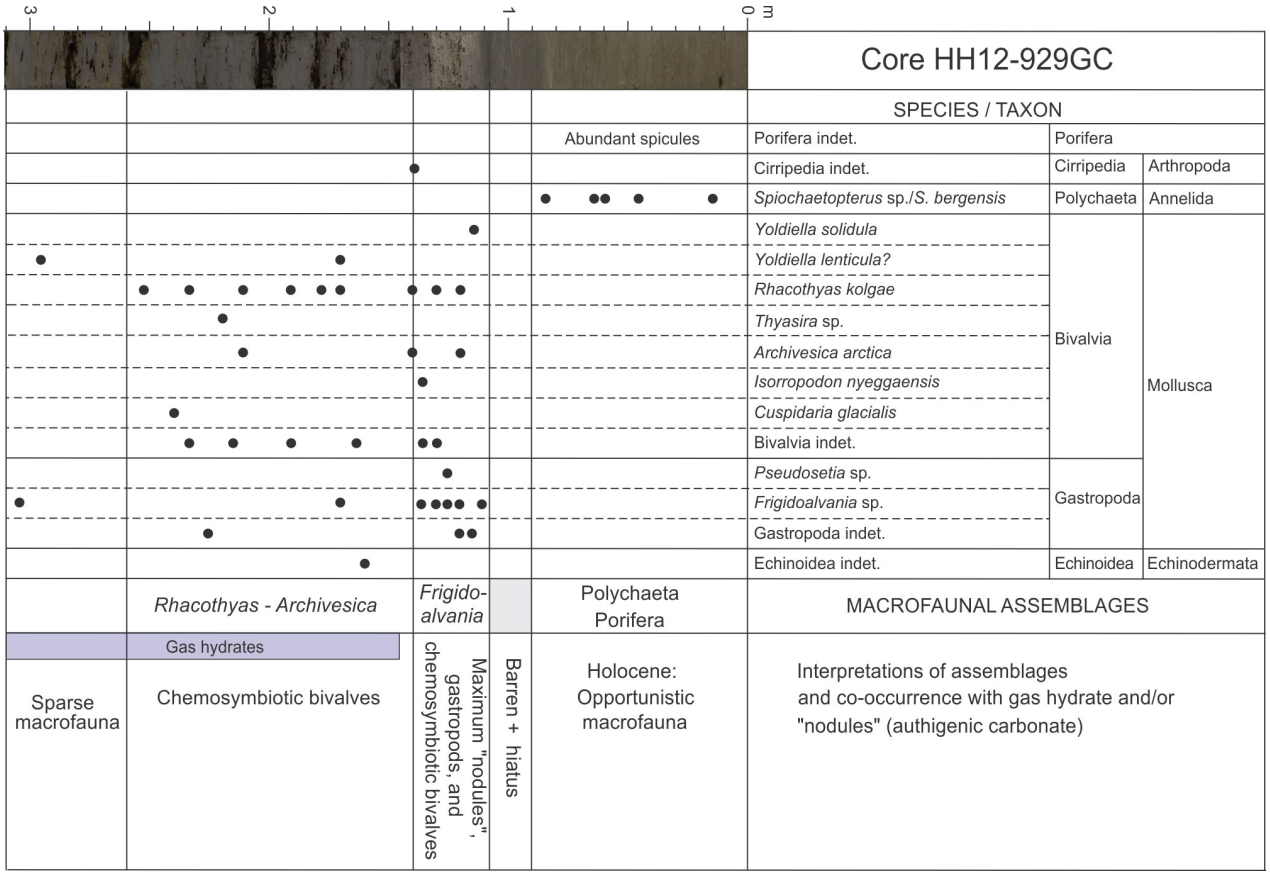

Fig. 7 Range chart of occurrence of macrofossils and trace fossils in core HH12-929GC.

In addition, rare Arctic infaunal bivalves *Yoldiella solidula* Warén, 1989, *Y. lenticula*(?) and *Cuspidaria glacialis* (Sars, 1878) have been recorded, as well as a few fragments of an undetermined cirriped at 140 cm (Fig. 7). All the small-sized bivalves are usually encrusted/coated with authigenic carbonate, making their systematics difficult to determine and somewhat uncertain.

From 110 to 90 cm no macrofossils were recorded, and there is a hiatus in the core (see above and Figs. 4, 5, 7). The topmost 90 cm, however, is characterized by abundant fragments of chitinous tubes from a benthic sedentary infaunal polychaete, *Spiochaetopterus* sp./*S. bergensis* Gitay, 1969, and other polychaetes (further identification of these has not been possible [E. Oug & J. Hansen, pers. comm. 2015]). Spicules of sponges are abundant in the same layer, in contrast to the layers below.

Interpretation: This core has been recovered from the deepest part of the pockmark and contains at least two macrofaunal assemblages (Fig. 7). The *Rhacothyas–Archivesica–Frigidoalvania* assemblage from 250 to 110 cm corresponds to MIS 3 and MIS 2, from about 45 100 to 21 000 years ago, and correlates to some extent with the presence of authigenic carbonate crust/nodules and overall peak low $\delta^{13}C$ values (Fig. 4). Together with other parameters, this indicates almost continuous, but variable, strong seepage of methane during the glacial period (Sztybor & Rasmussen 2017a). *Rhacothyas kolgae* is the most abundant bivalve in the record and is believed to be chemosymbiotic (Åström et al. 2017; Figs. 4, 6b, 7). It has so far only been recorded at shelf sites, but now it is also recorded as abundant in deepwater glacial sediments, together with other chemosymbiotic species (*A. arctica* and *I. nyeggaensis*). The presence of the small-sized infaunal bivalves *Y. solidula* and *C. glacialis* suggests an Arctic environment, as expected in the mid-late Weichselian (MIS 3–MIS 2). Authigenic carbonate nodules and ice-rafted debris are common and provide a hard substrate for the small epifaunal rissoid gastropods (Ponder 1984), especially *Frigidoalvania* sp. (Figs. 4, 7; Supplementary Note 3). This may explain why they are most common in this period. The entire deglacial period (ca. 21 000–9000 years ago) is missing in this record.

The polychaete–poriferan assemblage is in the topmost 90 cm of the core, comprising the mid- and late Holocene. The assemblage is typical for an opportunistic macrofauna after a major environmental disturbance (see Thomsen

Citation: *Polar Research* 2019, *38*, 3310, http://dx.doi.org/10.33265/polar.v38.3310

& Vorren 1986). This event may have been a blow-out, considering the position of the core in the deepest part of the pockmark and the presence of a hiatus.

Core HH12-928PC from the pavement area in the pockmark. The aragonitic pavement in the topmost few centimetres has encrusted shells of whole individuals of *Archivesica arctica* (Figs. 2, 4, 8; see also figure 3a in Sztybor & Rasmussen 2017a). Below the pavement, the authigenic carbonates occur in the lining of burrows and perhaps feeding tubes of a larger infaunal thyasirid bivalve, for example, *Rhacothyas kolgae* (see description and figures 4 and 5 in Oliver & Killeen 2002) and as encrustations/coatings of mollusc shells and as carbonate nodules.

Fragments of tubes of the polychaete *Spiochaetopterus* sp./*S. bergensis* and other polychaetes are very common throughout the core (from near the bottom to the top), as are specimens of *Y. solidula*, *Yoldiella* sp. and *A. arctica*. *Rhacothyas kolgae* is present (Figs. 6b, 8), but gastropods *Alvania scrobiculata* (Møller, 1842), *Frigidoalvania* sp., *Pseudosetia* sp. and *Skenea* sp. dominate the assemblage (Fig. 8). Many of the fossils in this core are difficult to deal with taxonomically because of encrustation/coating by the authigenic carbonate. The trace fossil *Oichnus* cf. *O. ovalis* Bromley, 1993 (Fig. 9; Supplementary Note 5) is recorded in shells of *Frigidoalvania* sp., indicating that they have been subjected to predatory gastropods (see Bromley 1993). The core also contains fragments of plates from echinoids and ossicles from ophiuroids (Supplementary Note 6), fragments of small beaks from cephalopods, a few scattered fragmentary bones from fishes and spicules from sponges—Cladorhizidae indet., *Stylocordyla* sp., Axenellidae indet., Demospongiae indet.—all are considered allochthonous and therefore cannot be used in an interpretation of the fauna.

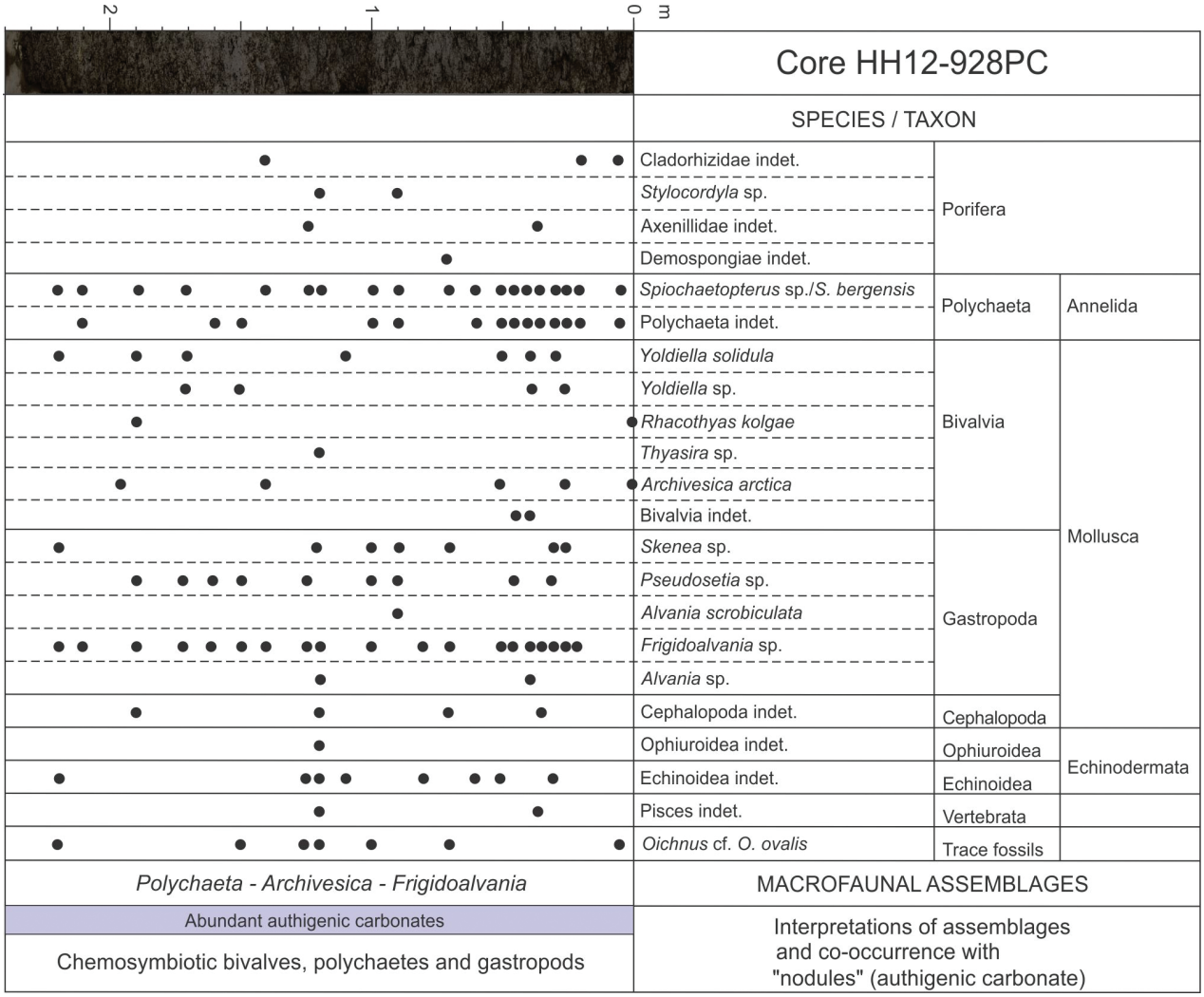

Fig. 8 Range chart of occurrence of macrofossils and trace fossils in core HH12-928PC.

Interpretation: This core is also from the pockmark and is completely dominated by one assemblage, a polychaete–*Archivesica*–*Frigidoalvania* assemblage (Fig. 8). With a rich assemblage of epifaunal and infaunal macrofauna, including a scattered occurrence of chemosymbiotic bivalves (Figs. 4, 6c, 7, 8), the fauna seems more diverse than that represented in core HH12-929GC. The low $\delta^{13}C$ values indicate methane seepage, which is confirmed by the presence of the chemosymbiotic macrofauna. The entire sequence appears to correlate with H1 (19 000–15 500 years ago) (Figs. 2, 4, 5).

Relationships between fossil macrofaunal assemblages, sedimentary environments and methane seepage

Analyses of the four cores from Vestnesa Ridge demonstrate the importance of a pockmark environment for the occurrence and distribution of benthic fossil macrofaunal assemblages in the deep Arctic Ocean. The core sequences show signs of methane seepage ranging from none (core JM10-333GC) through mainly moderate (JM10-335GC) and strong (HH12-929GC), to very strong (HH12-928PC) (Sztybor & Rasmussen 2017a; Fig. 2). Although variable through time, this overall gradient in influence of seepage is demonstrated by multiple palaeo-proxies, here exemplified by the benthic $\delta^{13}C$ records, the lithology and the presence of authigenic carbonate nodules (Figs. 3, 4). The finding of increasing density and diversity of preserved fossil macrofaunas with increasing methane influence in the four records shows that palaeo-seeps also constituted "oases" for the macrofaunas (see Åström et al. 2018) recurrently during the last 45 000 years or so (Figs. 3–10).

Glacial records (>19 000 years). The control core JM10-333GC was taken from outside the investigated pockmark (Fig. 1). It has not been subjected to seepage and contains no preserved fossil macrofauna, but rather a rich and well-preserved foraminiferal fauna (Sztybor & Rasmussen 2017b). As the core was collected from a non-seep site, its lack of chemosymbiotic species is to be expected. Considering the depth—about 1200 m—and location in the High Arctic, one should not expect a prolific macrofauna either, according to previous and new results on deep-sea Arctic macrofaunas (Åström et al. 2016 and references therein; Åström et al. 2018).

Core JM10-335GC was recovered from a fairly undisturbed part of the pockmark. The glacial stages MIS 3–MIS 2 show $\delta^{13}C$ values within the normal range and episodes of slightly lower values (Figs. 2, 3). There are no authigenic carbonates. Macrofaunas are confined to two thin layers. This is in contrast to core HH12-929GC, which is from the deepest part of the pockmark and which contained gas hydrates in the lower glacial part. The $\delta^{13}C$ values are mostly very low compared to core JM10-335GC, and carbonate nodules are very common, indicating strong seepage overall (Fig. 4). The core's fairly rich fossil macrofauna, characterized by the chemosymbiotic bivalves, *A. arctica* and *I. nyeggaensis*, indicates tolerance to the periodically moderate to strong seepage during MIS 3–MIS 2 (Figs. 4, 7). The most persistent species is the potentially chemosymbiotic thyasirid bivalve *R. kolgae*, occurring from ca. 33 000 to 21 000 years ago, according to the age model. It is apparently most abundant in coarser grained samples and to some extent in samples with high number of calcareous nodules (Fig. 4), indicating that it may have preferred coarser sediment. Similar to the vesicomyids, it appears to have tolerated moderate to strong seeping. The species has previously been located in methane seep sites of strong seepage in coarse sediments on the shelf off western Svalbard (Åström et al. 2016; Åström et al. 2017). The richest assemblage—with abundant *Frigidoalvania* sp.—occurs in the layer of highly concentrated carbonate nodules precipitated during the late Last Glacial Maximum about 21 000 years ago (Figs. 4, 7). This epifaunal species was probably likewise attracted to the coarse sediment that provided a secondary hard substrate (see section: Deglacial records 19 000–11 000 years from the pockmark).

MIS 3 sediments at the Svalbard margin (and elsewhere) generally show a high variability in planktic foraminiferal distribution patterns and concentrations, and in planktic oxygen isotope values (Dokken & Hald 1996; Rasmussen et al. 2014). Therefore, the part of the core that contained gas hydrates (older than ca. 21 500 years according to the age model; Figs. 2, 5) with the almost constant values of number/g of foraminifera and stable isotope ratios indicates mixing of the foraminifera in this interval (Figs. 4, 7). The mixing may have occurred as a result of strong upward fluid flow or from the dissociation of the hydrates during and after coring.

Deglacial records 19 000–11 000 years ago from the pockmark. In core JM10-335GC, *A. arctica* and *I. nyeggaensis* are found in two narrow horizons correlating in time with H1 (Figs. 2, 3). The layers of vesicomyid bivalves in the core may be explained by the occurrence of dissolved gas in the sediment below and the autecology of the bivalves. Vesicomyid bivalves inhabit sites that provide suitable amounts of reduced compounds (H_2S) for their autotrophic symbionts (e.g., Barry et al. 1997; Krylova & von Cosel 2011; Hansen et al. 2017; Olu et al. 2017). The dependence on H_2S concentration varies among species (Barry et al. 1997; Decker et al. 2017), but low concentrations and weak methane seepage may sustain some vesicomyid species (Decker et al. 2012; Pop Ristova et al. 2012), while very high concentrations may be lethal (Sahling et al. 2003;

Citation: *Polar Research* 2019, *38*, 3310, http://dx.doi.org/10.33265/polar.v38.3310

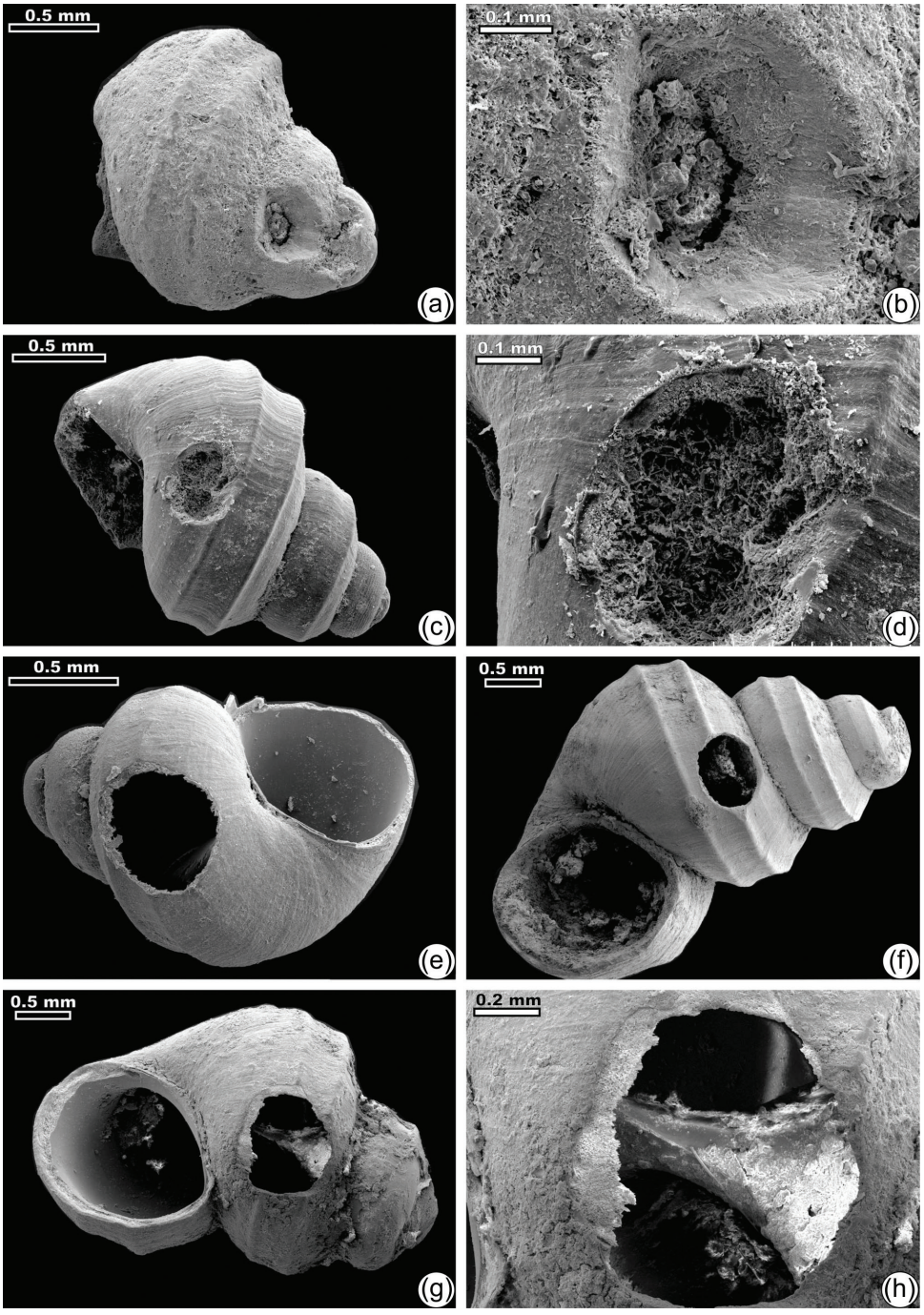

Fig. 9 Gastropods, (a)-(d) and (f)-(h) *Frigidoalvania* sp. and (e) an undetermined species, with three forms—A, B and C—of the trace fossil *Oichnus* cf. *O. ovalis* Bromley, 1993, from core HH12-928PC. (a) Form A, (b) is the detail of (a); (c) Form B, (d) is the detail of (c); (e, f, g) Form C, (h) is the detail of (g). For detailed information see Supplementary Note 5.

Heyl et al. 2007). It is known from investigations of recent vesicomyids that they live as infauna, and depending on their ability to bind oxygen, they can move up and down into the sediment (Decker et al. 2014; Krylova & von Cosel 2011; Decker et al. 2017; Olu et al. 2017). They occur in clusters that are distributed over large areas (Sahling et al. 2002; Levin et al. 2003; Treude et al. 2003; Menot et al. 2010). The occurrence of these bivalves as a layer in the core implies either that they are allochthonous or that the bivalves are in situ opportunists. They (and

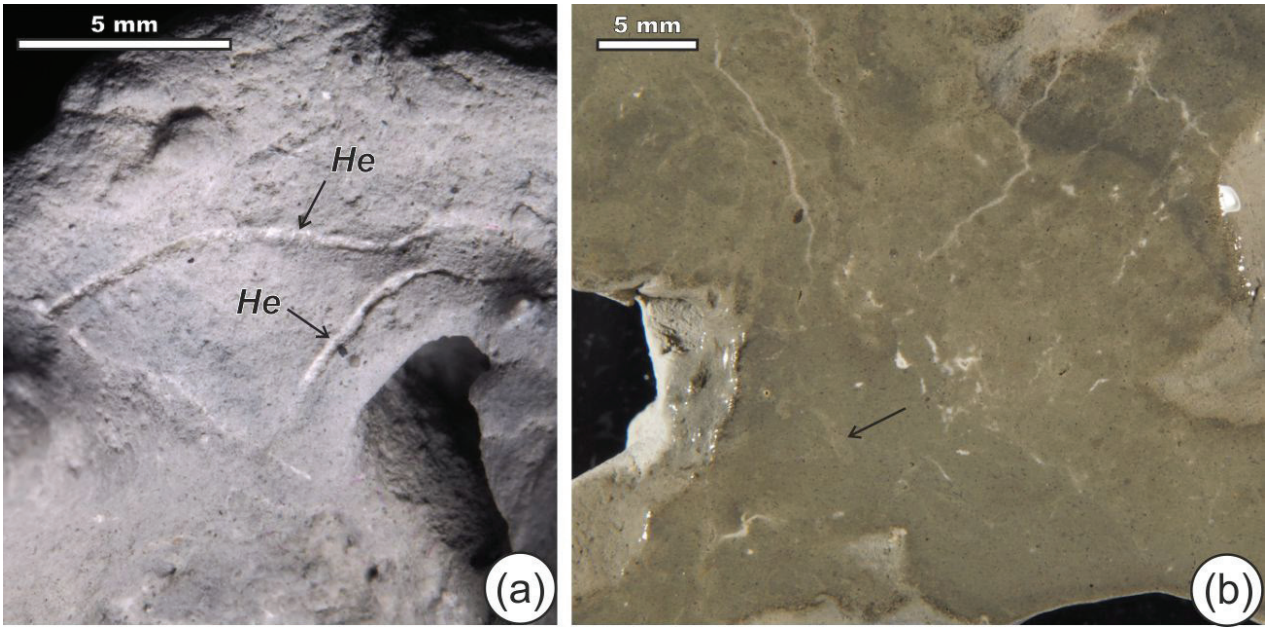

Fig. 10 Ichnological features of the concretions/nodules from core HH12-929GC, 195–192 cm. (a) Thin, winding burrows, *Helminthoidichnites* isp., on the surface (arrows). (b) Polished surface displays cross-section of small burrows filled with sediment (arrow) and shows ichnofabric transformed partly by diagenesis.

other chemosymbiotic bivalve species) have been located in similar concentrated layers in several core records, of similar age, from different pockmarks at Vestnesa Ridge (Sztybor et al. 2013; Ambrose et al. 2015; Myrvang 2016; Hansen et al. 2019). Their presence has been related to the increased bottom water temperatures that occur during H1 (Sztybor & Rasmussen 2017b; Hansen et al. 2017). The finding of a new solemyid species of *Acharax* from the same and neighbouring pockmarks at Vestnesa Ridge, also of H1 age, supports this. Both fossil and modern *Acharax* species also occur at lower latitudes (Hansen et al. 2019 and references therein). The chemosymbiotic bivalves disappear at the start of the Bølling interstadial when bottom water cooled abruptly (e.g., Ezat et al. 2014 and references therein). This cooling may have been the most likely cause of their demise; alternatively, the inferred increase in seepage from the start of the Bølling interstadial may have reached a lethal level. It should be mentioned that none of the chemosymbiotic species *A. arctica*, and *I. nyeggaensis* has so far been recorded alive in seep sites at Vestnesa or elsewhere in the Nordic seas and Arctic Ocean (see discussion and references in Hansen et al. 2017; Hansen et al. 2019). The same applies for *R. kolgae* (Åström et al. 2017; Åström et al. 2018). The presence of vesicomyid/solemyid layers in H1 therefore most likely do not indicate a maximum in seepage as postulated by, for example, Ambrose et al. (2015) and Schneider et al. (2017), but rather higher bottom water temperatures at the time.

Core HH12-928PC was recovered from an elevated aragonitic pavement area, presumably representing the most intense seeping in the pockmark (Figs. 2, 4). Here we find *A. arctica* not in confined layers as in core JM10-335GC (Fig. 2), but as single specimens throughout the record (Fig. 8). The record is also very disturbed from the growth of numerous authigenic carbonates, probably causing a pronounced expansion of the sediment record, given the short time interval it represents (H1, 19 000–15 500 years ago; Fig. 5). The $\delta^{13}C$ values in *C. neoteretis* are very low throughout, while the epibenthic species *C. wuellerstorfi* yields $\delta^{13}C$ values within the "normal" range in some intervals, which could indicate events of lower activity.

Core HH12-928PC is the record with the highest diversity and abundance of gastropods and of *Frigidoalvania* sp. (Fig. 8). As hard substrates, the carbonate concretions are of importance for a vagile epifauna of deposit feeding gastropods, in particular rissoids, for example, *Frigidoalvania* sp., and carnivorous naticids that prey on the rissoids. The latter are documented by the trace fossil *Oichnus* (Fig. 9; Supplementary Note 5). The presence of epifaunal gastropod species shows that they must be capable of surviving and/or even benefitting from the seep environment offering both food and a secondary hard substrate as at ca. 21 000 years ago in core HH12-929GC. Recent gastropods are in general very abundant in both microbial mats and siboglinid fields at cold seeps on the Norwegian margin (Decker et al. 2012) and $\delta^{13}C$

Citation: *Polar Research* 2019, *38*, 3310, http://dx.doi.org/10.33265/polar.v38.3310

ratios in *Alvania* sp. were shown to reach very low values (below −40‰), indicating that they feed and calcify in seep environments (Decker & Olu 2012).

In core HH12-929GC, a hiatus comprising the entire interval from the late glacial to the earliest Holocene (ca. 21 000–9000 years ago) suggests that a blow-out may have occurred in this deepest part of the pockmark, where core HH12-929GC was retrieved. This timing of a maximum in seepage accords well with previous studies from a number of pockmarks from Vestnesa Ridge based on ^{13}C isotopes and other proxies (e.g., Consolaro et al. 2015; Sztybor & Rasmussen 2017a).

Holocene faunas from the pockmark. Holocene sediments are only present in cores JM10-335GC and HH12-929GC (Fig. 5). In core JM10-335GC, the Holocene mud in the topmost 40 cm of the core dates from the early Holocene and—dominated by abundant sponges (spicules)—contains a fauna entirely different from the glacial period. We anticipated that sponge spicules would be common in our samples because they are also common in North Atlantic deepwater sediments (see, e.g., Barthel & Tendal 1993 and Klitgaard & Tendal 2004 for overviews). Photographic surveys (Soltwedel et al. 2009; Bergmann, Langwald et al. 2011; Bergmann, Soltwedel et al. 2011) and Agassiz trawl and bottom trawl hauls (Piepenburg et al. 1996; Bergmann et al. 2009) of the sponge fauna west of Svalbard indicate a rather rich sponge fauna both on the shelf and on the slope south-west of Vestnesa Ridge. The spicules occur partly in a layer of mud containing abundant diatoms dating to ca. 10 000 years ago (e.g., Jessen et al. 2010; Fig. 2). The event has been interpreted as one of increased productivity due to the northward passing of the Arctic Front in the early Holocene (see Jessen et al. 2010 and references therein). The high supply of food particles to the seafloor may have sustained an apparently rich community of sponges.

Living siboglinid polychaetes have been sampled from the seabed at site JM10-335GC and possibly site HH12-929GC. These polychaetes have previously been associated with seep environments (see e.g., Niemann et al. 2006; Åström et al. 2016; Sen et al. 2018; Sen et al. 2019) and are therefore important for the interpretation of the present environment of active cold seepage. The $\delta^{13}C$ values in JM10-335GC for the Holocene are slightly lower than "normal" for Holocene sediments (Fig. 3), also pointing to an influence of methane seeping. Most of the Holocene in core HH12-929GC has high $\delta^{13}C$ values, as seen in the epibenthic species *C. lobatulus* (Fig. 4). Unfortunately, the endobenthic species *C. neoteretis* was too rare for isotopic analysis. However, *M. barleeanus* shows $\delta^{13}C$ values below −4‰, indicating an influence of seepage (Sztybor & Rasmussen 2017a). The disappearance of the chemosymbiotic bivalves, *A. archivesica* and *I. nyeggaensis,* is probably due to the cold bottom water conditions (section: Deglacial records 19 000–11 000 years from the pockmark). The deposition of fine mud during the Holocene and the lack of coarse ice-rafted debris and encrustations can probably explain the absence of *R. kolgae* and the seep-associated species (gastropods) that all appear to be linked to coarser sediments. The general absence of hard-shelled fossils in the Holocene sediments indicates that they were rare and that most of the macrofaunas were soft-bodied, as are most of the faunas at seep sites today (Åström et al. 2016; Åström et al. 2018).

Conclusions

The distribution patterns of macrofaunas in four marine core records from a pockmark field on Vestnesa Ridge in Fram Strait, western Svalbard margin, were investigated, supported by data from foraminifera, stable isotopes and sedimentological data. One core was from outside the pockmarks, and three cores were from within an active pockmark with seeping of methane. The investigations of the four cores have confirmed a close relationship between fossil macrofaunal assemblages with chemosymbiotic bivalves, polychaetes and epifaunal gastropods and authigenic carbonates/gas seepage. Also, an environmental event, possibly a blow-out, in one of the cores (HH12-929GC) resulted in a hiatus from ca. 21 000 to ca. 9000 years ago. The presence of living chemosymbiotic polychaetes (siboglinids) in the topmost part of a core (JM10-335GC) from inside the pockmark confirms an active seepage from the pockmark.

The results show a major difference between the macrofaunas recovered from the area outside the pockmark with no methane seepage and with no preserved macrofauna compared to records from within the active pockmark. In the record with moderate seepage, chemosymbiotic macrofaunas (vesicomyids) were confined to two layers correlating with H1, 19 000–15 500 years ago. Otherwise, the record is barren of macrofauna, except for sponge spicules in the upper Holocene part and living siboglinid polychaetes in the top layer. The record of strong seepage from the deepest part of the pockmark shows a scattered macrofauna of thyasirids, rissoid gastropods and vesicomyids. The record from an area of the pockmark with aragonitic pavement and severe encrustations in and on the sediment and with maximum seepage shows maximum diversity and density of macrofaunas. Here, few thyasirids but abundant vesicomyids and a very high abundance of polychaetes (as fragments of tubes from, e.g., *Spiochaetopterus* sp.) and rissoid gastropods were found, the latter mainly dominated by deposit feeding *Frigidoalvania* sp. The distribution of fossil

macrofaunas from the four records of different degrees of influence of methane seepage confirms earlier studies of modern faunas in that seepage for the most part appears advantageous for macrofaunal density and diversity in the deep sea. Arctic seeps at Vestnesa Ridge in the eastern Fram Strait constituted oases for macrofaunas recurrently during the last ca. 45 000 years as they do today.

Acknowledgements

We thank the captain and crew of the RV *Helmer Hanssen* for taking the gravity cores and engineer S. Iversen for help with piston coring, data acquisition and handling. The late Jon-Arne Sneli (Norwegian University of Science and Technology), Jesper Hansen (Akvaplan-niva) and Eivind Oug (Norwegian Institute for Water Research) commented on the identification of molluscs and polychaetes. Thanks are also due to S. Vadakkepuliyambatta for help with Fig. 1b. Torger Grytå (UiT—The Arctic University of Norway) drew Figs. 7 and 8. Mari Karlstad (The Arctic University Museum of Norway, UiT—The Arctic University of Norway) took the photographs of the bivalves in Fig. 6. Karine Olu and an anonymous reviewer are warmly thanked for their very helpful reviews of the manuscript.

Disclosure statement

The authors report no conflict of interest.

Funding

This research was funded by a Mohn Foundation, UiT—The Arctic University of Norway, grant to the Paleo-CIRCUS project 2010–2014. The project received further funding from the Research Council of Norway through its Centres of Excellence funding scheme (project no. 223 259). The publication also received support from the publication fund of UiT—The Arctic University of Norway.

References

Aagard K., Foldvik A. & Hillman S.R. 1987. The West Spitsbergen Current: disposition and water mass transformation. *Journal of Geophysical Research—Oceans 92*, 3778–3784, http://dx.doi.org/10.1029/JC092iC04p03778.

Ambrose W.G., Panieri G., Schneider A., Plaza-Faverola A., Carroll M.L., Åström E.K.L., Locke W.L. & Carroll J. 2015. Bivalve shell horizons in seafloor pockmarks of the last glacial–interglacial transition: a thousand years of methane emissions in the Arctic Ocean. *Geochemistry, Geophysics, Geosystems 16*, 4108–4129, http://dx.doi.org/10.1002/2015GC005980.

Åström E.K.L., Carroll M.L., Ambrose W.G. Jr. & Carroll J. 2016. Arctic cold seep in marine methane hydrate environments: impacts on shelf microbenthic community structure offshore Svalbard. *Marine Ecology Progress Series 552*, 1–18, http://dx.doi.org/10.3354/meps11773.

Åström E.K.L., Carroll M.L., Ambrose W.G. Jr., Sen A., Silyakova A. & Carroll J. 2018. Methane cold seeps as biological oases in the High-Arctic deep sea. *Limnology and Oceanography 63*, S209–S231, http://dx.doi.org/10.1002/lno.10732.

Åström E.K.L., Oliver P.G. & Carroll M.L. 2017. A new genus and two new species of Thyasiridae associated with methane seeps off Svalbard, Arctic Ocean. *Marine Biology Research 13*, 402–416, http://dx.doi.org/10.1080/17451000.2016.1272699.

Barry J.P., Kochevar R.E. & Baxter C.H. 1997. The influence of pore-water chemistry and physiology on the distribution of vesicomyid clams of cold seeps in Monterey Bay: implications for patterns of chemosynthetic community organization. *Limnology and Oceanography 42*, 318–328, http://dx.doi.org/10.4319/lo.1997.42.2.0318.

Barthel D. & Tendal O.S. 1993. The sponge association of the abyssal Norwegian–Greenland Sea: species composition, substrate relationships and distribution. *Sarsia 78(2)*, 83–96, http://dx.doi.org/10.1080/00364827.1993.10413524.

Bergmann M., Dannheim J., Bauerfeind E. & Klages M. 2009. Trophic relationships along a bathymetric gradient at the deep-sea observatory Hausgarten. *Deep-Sea Research Part I 56*, 408–424, http://dx.doi.org/10.1016/j.dsr.2008.10.004.

Bergmann M., Langwald N., Ontrup J., Soltwedel T., Scheve I., Klages M. & Nattkemper T.W. 2011. Megafaunal assemblages from two shelf stations west of Svalbard. *Marine Biology Research 7*, 525–539, http://dx.doi.org/10.1080/17451000.2010.535834.

Bergmann M., Soltwedel T. & Klages M. 2011. The interannual variability of megafaunal assemblages in the Arctic deep sea: preliminary results of the Hausgarten observatory (79°N). *Deep-Sea Research Part I 58*, 711–723, http://dx.doi.org/10.1016/j.dsr.2011.03.007.

Boetius A., Ravenschlag K., Schubert C.J., Rickert D., Widdel F., Gieseke A., Amann R., Jorgensen B.B., Witte U. & Pfannkuche O. 2000. A marine microbial consortium apparently mediating anaerobic oxidation of methane. *Nature 407*, 623–626, http://dx.doi.org/10.1038/35036572.

Bond G., Broecker W., Johnsen S., McManus J., Labeyrie L., Jouzel J. & Bonani G. 1993. Correlations between climate records from the North Atlantic sediments and Greenland ice. *Nature 365*, 143–147, http://dx.doi.org/10.1038/365143a0.

Borowski W.S., Paull C.K. & Ussler W. 1996. Marine pore-water sulphate profiles indicate in situ methane flux from underlying gas hydrate. *Geology 24*, 655–658, http://dx.doi.org/10.1130/0091-7613(1996)024<0655:MPWSPI>2.3.CO;2.

Bromley R.G. 1993. Predation habits of octopus past and present and a new ichnospecies *Oichnus ovalis*. *Bulletin of the Geological Society of Denmark 40*, 167–173.

Brooks J.M., Kennicutt M.C., Fisher C.R., Macko S.A., Cole K. Childress J.J., Bidigare R.R. & Vetter R.D. 1987. Deep-sea hydrocarbon seep communities: evidence for energy

and nutritional carbon sources. *Science 238*, 1138–1142, http://dx.doi.org/10.1126/science.238.4830.1138.

Bünz S., Polyanov S., Vadakkepuliyambatta S., Consolaro C. & Mienert J. 2012. Active gas venting through hydrate-bearing sediments on the Vestnes Ridge, offshore W-Svalbard. *Marine Geology 332–334*, 189–197, http://dx.doi.org/10.1016/j.margeo.2012.09.012.

Consolaro C., Rasmussen T.L., Panieri G., Mienert J., Buenz S. & Sztybor K. 2015. Carbon isotope ($\delta^{13}C$) excursions suggest times of major methane release during the last 14 ka in Fram Strait, the deep-water gateway to the Arctic. *Climate of the Past 11*, 669–685, http://dx.doi.org/10.5194/cp-11-669-2015.

Cook M.S., Keigwin L.D., Birgel D. & Hinrichs K.-U. 2011. Repeated pulses of vertical methane flux recorded in glacial sediments from the southeast Bering Sea. *Paleoceanography 26*, PA2210, http://dx.doi.org/10.1029/2010PA001993.

Decker C., Morineaux M., van Gaever S., Caprais J.-C., Lichtschlag A., Gauthier O., Andersen A.C. & Olu K. 2012. Habitat heterogeneity influences cold-seep macrofaunal communities within and among seeps along the Norwegian margin. Part 1: macrofaunal community structure. *Marine Ecology 33*, 205–230, http://dx.doi.org/10.1111/j.1439-0485.2011.00503.x.

Decker C. & Olu K. 2012. Habitat heterogeneity influences cold-seep macrofaunal communities within and among seeps along the Norwegian margin. Part 2: contribution of chemosynthesis and nutritional patterns. *Marine Ecology 33*, 231–245, http://dx.doi.org/10.1111/j.1439-0485.2011.00486.x.

Decker C., Zorn N., Le Bruchec J., Caprais J.-C., Potier N., Leize-Wagner E., Lallier F.H., Olu K. & Andersen A.C. 2017. Can the haemoglobin characteristics of vesicomyid clam species influence their distribution in deep-sea sulfide-rich sediments? A case study in the Angola Basin. *Deep-Sea Research Part II 142*, 219–232, http://dx.doi.org/10.1016/j.dsr2.2016.11.009.

Decker C., Zorn N., Potier N., Leize-Wagner E., Lallier F.H. & Olu K. 2014. Globin's structure and function in vesicomyid bivalves from the Gulf of Guinea cold seeps as an adaptation to life in reduced sediments. *Physiological and Biochemical Zoology 87*, 855–869, http://dx.doi.org/10.1086/678131.

Dokken T. & Hald M. 1996. Rapid climatic shifts during isotope stages 2–4 in the polar North Atlantic. *Geology 24*, 599–602, http://dx.doi.org/10.1130/0091-7613(1996)024<0599:RCSDIS>2.3.CO;2.

Duplessy J.C., Shackleton N.J., Fairbanks R.G., Labeyrie L., Oppo D. & Kallel N. 1988. Deepwater source variations during the last climatic cycle and their impact on the global deepwater circulation. *Paleoceanography 3*, 343–360, http://dx.doi.org/10.1029/PA003i003p00343.

Eiken O. & Hinz K. 1993. Contourites in the Fram Strait. *Sedimentary Geology 82*, 15–32, http://dx.doi.org/10.1016/0037-0738(93)90110-Q.

Ezat M., Rasmussen T.L. & Groeneveld J. 2014. Persistent intermediate water warming during cold stadials in the southeastern Nordic seas during the past 65 k.y. *Geology 42*, 663–666, http://dx.doi.org/10.1130/G35579.1.

Fisher R.E., Sriskantharajah S., Lowry D., Lanoisellé M., Fowler C.M.R., James R.H., Hermansen O., Lund Myhre C., Stohl A., Greinert J., Nisbet-Jones P.B.R., Mienert J. & Nisbet E.G. 2011. Arctic methane sources: isotopic evidence for atmospheric input. *Geophysical Research Letters 38*, L21803, http://dx.doi.org/10.1029/2011GL049319.

Fontanier C., Koho K.A., Goñi-Urizza M.S., Deflandre B., Galaup S., Ivanovsky A., Gayet N., Dennielou B., Crémare A., Bichon S., Gassie C., Anschutz P., Duran R. & Reichart G.J. 2014. Benthic foraminifera from the deep-water Niger delta (Gulf of Guinea): assessing present-day and past activity of hydrate pockmarks. *Deep-Sea Research Part I 94*, 87–106, http://dx.doi.org/10.1016/j.dsr.2014.08.011.

Hansen J., Ezat M.M., Åström E.K.L. & Rasmussen T.L. 2019. New Late Pleistocene species of *Acharax* from Arctic methane seeps off Svalbard. *Journal of Systematic Palaeontology*, early access, http://dx.doi.org/10.1080/14772019.2019.1594420.

Hansen J., Hoff U., Sztybor K. & Rasmussen T.L. 2017. Taxonomy and palaeoecology of two Late Pleistocene species of vesicomyid bivalves from cold methane seeps at Svalbard (79°N). *Journal of Molluscan Studies 3*, 270–279, http://dx.doi.org/10.1093/mollus/eyx014.

Heyl T.P., Gilhooly W.P., Chambers R.M., Gilchrist G.W., Macko S.A., Ruppel C.D. & Van Dover C.L. 2007. Characteristics of vesicomyid clams and their environment at the Blake Ridge cold seep, South Carolina, USA. *Marine Ecology Progress Series 339*, 169–184, http://dx.doi.org/10.3354/meps339169.

Hill T.M., Paull C.K. & Crister R.B. 2012. Glacial and deglacial seafloor methane emissions from pockmarks on the northern flank of the Storegga Slide complex. *Geo-Marine Letters 32*, 73–84, http://dx.doi.org/10.1007/s00367-011-0258-7.

Hong W.-L., Sauer S., Pameri G., Ambrose W.G. Jr., James R.H., Plaza-Faverola A. & Schneider A. 2016. Removal of methane through hydrological, microbial, and geochemical processes in the shallow sediments of pockmarks along eastern Vestnesa Ridge (Svalbard). *Limnology and Oceanography 61*, 324–343, http://dx.doi.org/10.1002/lno.10299.

Hopkins J.S. 1991. The GIN Sea—A synthesis of its physical oceanography and literature review 1972–1985. *Earth Science Reviews 30*, 175–318, http://dx.doi.org/10.1016/0012-8252(91)90001-V.

Hovland M. 2008. *Deep-water coral reefs. Unique biodiversity hot-spots*. Chichester, UK: Springer.

Hovland M. & Thomsen E. 1989. Hydrocarbon based communities in the North Sea? *Sarsia 74*, 29–42, http://dx.doi.org/10.1080/00364827.1989.10413420.

Howe J.A., Shimmield T.M. & Harland R. 2008. Late Quaternary contourites and glaciomarine sedimentation in the Fram Strait. *Sedimentology 55*, 179–200, http://dx.doi.org/10.1111/j.1365-3091.2007.00897.x.

Hustoft S., Bünz S., Mienert J. & Chand S. 2009. Gas hydrate reservoir and active methane-venting province in sediments on <20 Ma young oceanic crust in the Fram Strait, offshore NW-Svalbard. *Earth and Planetary Science Letters 284*, 12–24, http://dx.doi.org/10.1016/j.epsl.2009.03.038.

Hustoft S., Dugan B. & Mienert J. 2009. Effects of rapid sedimentation on developing the Nyegga

pockmark field: constraints from hydrological modeling and 3-D seismic data, offshore mid-Norway. *Geochemistry, Geophysics, Geosystems 10*, Q06012, http://dx.doi.org/10.1029/2009GC002409.

Jessen S.P., Rasmussen T.L., Nielsen T. & Solheim A. 2010. A new Late Weichselian and Holocene marine chronology for the western Svalbard slope 30,000-0 cal. years BP. *Quaternary Science Reviews 29*, 1301–1312, http://dx.doi.org/10.1016/j.quascirev.2010.02.020.

Klitgaard A.B. & Tendal O.S. 2004. Distribution and species composition of mass occurrences of large-sized sponges in the northeast Atlantic. *Progress in Oceanography 61*, 57–98, http://dx.doi.org/10.1016/j.pocean.2004.06.002.

Krylova E.M., Gebruk A.V., Portnova D.A., Todt C. & Hafliidason H. 2001. New species of the genus *Isorropodon* (Bivalvia: Vesicomyidae: Pliocardiinae) from cold methane seeps at Nyegga (Norwegian Sea, Vøring Plateau, Storegga Slide). *Journal of the Marine Biological Association of the United Kingdom 91*, 1135–1144, http://dx.doi.org/10.1017/S002531541100004X.

Krylova E.M. & von Cosel R. 2011. A new genus of large Vesicomyidae (Mollusca, Bivalvia, Vesicomyidae, Pliocardiinae) from the Congo margin, with the first record of the subfamily Pliocardiinae in the Bay of Biscay (northeastern Atlantic). *Zoosystema 33*, 83–99, http://dx.doi.org/10.5252/z2011n1a4.

Laier T., Rasmussen T.L., Sztybor K. & Nielsen T. 2017. Gas migration through a 150 m hydrate stability zone off Svalbard results in local shallow 'secondary' hydrate formation. Poster presented at the 9th International Conference on Gas Hydrates, 25–30 June, Denver, CO.

Lartaud F., de Rafelis M., Oliver G., Krylova E., Dymnet J., Ildefonse B., Thibaus R., Gente P., Hoisé E., Meistertzheim A.-L., Fouquet Y. Gaill F. & le Bris N. 2010. Fossil clams from a serpentinite-hosted sedimented vent field near the active smoker complex Rainbow, MAR, 36 13´N: insight into the biography of vent fauna. *Geochemistry, Geophysics, Geosystems 11*, Q0AE01, http://dx.doi.org/10.1029/2010GC003079.

Levin L. 2005. Ecology of cold seep sediments: interactions of fauna with flow, chemistry and microbes. In R.N. Gibson et al. (eds.): *Oceanography and marine biology. An annual review. Vol. 43*. Pp. 1–46. Boca Raton, FL: Taylor & Francis.

Levin L.A., Ziebis W., Mendoza G.F., Growney V.A., Tryons M.D., Brown K.M., Mahn C., Gieske J.M. & Rathburn A.E. 2003. Spatial heterogeneity of macrofauna at northern California methane seeps: influence of sulfide concentration and fluid flow. *Marine Ecology Progress Series 265*, 123–130, http://dx.doi.org/10.3354/meps265123.

Lisiecki L.E. & Raymo M.E. 2005. A Pliocene–Pleistocene stack of 57 globally distributed benthic $\delta^{18}O$ records. *Paleoceanography 20*, PA1003, http://dx.doi.org/10.1029/2004PA001071.

MacDonald I.R., Boland G.S., Baker J.S., Brooks J.M., Kennicutt M.C. & Bidigare R.R. 1989. Gulf of Mexico hydrocarbon seep communities. *Marine Biology 101*, 235–247, http://dx.doi.org/10.1007/BF00391463.

Marcon Y., Sahling H., Allais A.-G., Borhmann G. & Olu K. 2014. Distribution and temporal variation of mega-fauna at the Regab pockmark (northern Congo Fan), based on a comparison of videomosaics and geographic information systems analyses. *Marine Ecology 35*, 77–95, http://dx.doi.org/10.1111/maec.12056.

Menot L., Galeron J., Olu K., Caprais J.C., Crassous P., Khripounoff, A. & Sibuet M. 2010. Spatial heterogeneity of macro-infaunal communities in and near a giant pockmark area in the deep Gulf of Guinea. *Marine Ecology 31*, 78–93, http://dx.doi.org/10.1111/j.1439-0485.2009.00340.x.

Myrvang K. 2016. *Correlation between changes in paleoceanography, paleoclimate and methane seepage on Vestnesa Ridge, eastern Fram Strait*. Master's thesis, Dept. of Geology, UiT—The Arctic University of Norway, Tromsø, Norway.

Niemann H., Losekann T., de Beer D., Elvert M., Nadalig T., Knittel K., Amann R., Sauter E.J., Klages M., Foucher J.P. & Boetius A. 2006. Novel microbial communities of the Håkon Mosby mud volcano and their role as a methane sink. *Nature 443*, 854–858, http://dx.doi.org/10.1038/nature05227.

Oliver P.G. & Killeen J.J. 2002. *The Thyasiridae (Mollusca: Bivalvia) of the British continental shelf and North Sea oilfields. An identification manual. BIOMÔR 3*. Cardiff: National Museums and Galleries of Wales.

Olu K., Decker C., Pastor L., Caprais J.-C., Khripounoff A., Morineaux M., Ain Baziz M., Menot L. & Rabobouille C. 2017. Cold-seep-like macrofaunal communities in organic- and sulphide-rich sediments of the Congo deep-sea fan. *Deep-Sea Research Part II 142*, 180–196, http://dx.doi.org/10.1016/j.dsr2.2017.05.005.

Olu K., Lance S., Sibuet M., Henry P., Fiala Medioni A. & Dinet A. 1997. Cold seep communities as indicators of fluid expulsion patterns through mud volcanoes seaward of the Barbados accretionary prism. *Deep-Sea Research Part I 44*, 811–841, http://dx.doi.org/10.1016/S0967-0637(96)00123-9.

Paull C.K., Hecker B., Commeau R., Freeman-Lynde R.P., Neumann C., Corso W.P., Golubic S., Hook J.E., Sikes E. & Curray J. 1984. Biological communities at the Florida Escarpment resemble hydrothermal vent taxa. *Science 226*, 965–967, http://dx.doi.org/10.1126/science.226.4677.965.

Petersen C.J., Bünz S., Hustoft J., Mienert J & Klaeschen D. 2010. High-resolution P-Cable 3D seismic imaging of gas chimney structures in gas hydrated sediments of an Arctic sediment drift. *Marine and Petroleum Geology 27*, 1981–1994, http://dx.doi.org/10.1016/j.marpetgeo.2010.06.006.

Piepenburg D., Chernova N.V., Dorrien C., Gutt J., Neyelov A.V., Rachor E., Saldanha L. & Schmid M.K. 1996. Megabenthic communities in the waters around Svalbard. *Polar Biology 16*, 431–446, http://dx.doi.org/10.1007/BF02390425.

Pimenov N.V., Savvichev A.S., Rusanov I.I., Lein A.Y. & Ivanov M.V. 2000. Microbiological processes of the carbon and sulfur cycles at cold methane seeps of the North Atlantic. *Microbiology 69*, 709–720, http://dx.doi.org/10.1023/A:1026666527034.

Plaza-Faverola A., Bünz S. Johnson J.E., Chand S., Knies J., Mienert J. & Franek P. 2015. Role of tectonic stress in seepage evolution along the gas hydrate-charged Vestnesa

Ridge, Fram Strait. *Geophysical Research Letters 42*, 733–742, http://dx.doi.org/10.1002/2014GL062474 .

Plaza-Faverola A. & Keiding M. 2019. Correlation between tectonic stress regimes and methane seepage on the western Svalbard margin. *Solid Earth 10*, 79–94, http://dx.doi.org/10.5194/se-10-79-2019.

Ponder W.F. 1984. *A review of the genera of the Rissoidae (Mollusca: Mesogastropoda: Rissoacea). Records of the Australian Museum Supplement 4*. Sydney: Australian Museum.

Pop Ristova P., Wenzhöfer F., Ramette A., Zabel M., Fischer D., Kasten S. & Boetius A. 2012. Bacterial diversity and biogeochemistry of different chemosynthetic habitats of the REGAB cold seep (West African margin, 3160 m water depth). *Biogeosciences 9*, 5031–5048, http://dx.doi.org/10.5194/bg-9-5031-2012.

Rasmussen T.L., Thomsen E. & Nielsen T. 2014. Water mass exchange between the Nordic seas and the Arctic Ocean on millennial time scale during MIS 4–MIS 2. *Geochemistry, Geophysics, Geosystems 15*, 530–544, http://dx.doi.org/10.1002/2013GC005020.

Reimer P.J., Bard E., Beck J.W., Baillie M.G.L., Blackwell P.G., Bronk Ramsey C., Buck C.E., Cheng H., Edwards R.L., Friedrich M., Grootes P.M., Guilderson T.P., Haflidason H., Hajdas I., Hatte M., Reimer R.W., Richards D.A., Scott E.M., Southon J.R., Staff R.A., Turney C.S.M. & van der Plicht J. 2013. IntCal13 and Marine13 radiocarbon age calibration curves, 0–50,000 years cal BP. *Radiocarbon 55*, 1869–1887, http://dx.doi.org/10.2458/azu_js_rc.55.16947.

Sahling H., Galkin S.V., Salyuk A., Greinert J., Foerstel H., Piepenburg D. & Suess E. 2003. Depth-related structure and ecological significance of cold-seep communities—a case study from the Sea of Okhotsk. *Deep-Sea Research Part I 50*, 1391–1409, http://dx.doi.org/10.1016/j.dsr.2003.08.004.

Sahling H., Rickert D., Lee D., Linke R.W. & Suess E. 2002. Macrofaunal community structure and sulfide flux at hydrate deposits from the Cascadia convergent margin, NE Pacific. *Marine Ecology Progress Series 231*, 121–138, http://dx.doi.org/10.3354/meps231121.

Schauer U., Fahrbach E., Osterhus S. & Rohardt G. 2004. Arctic warming through the Fram Strait: oceanic heat transport from 3 years of measurements. *Journal of Geophysical Research—Oceans 109*, C06026, http://dx.doi.org/10.1029/2003JC001823.

Schneider A., Crémiere A., Panieri C., Lepland A. & Knies J. 2017. Diagenetic alteration of benthic foraminifera from a methane seep site on Vestnesa Ridge (NW Svalbard). *Deep-Sea Research Part I 123*, 22–34, http://dx.doi.org/10.1016/j.dsr.2017.03.001.

Sen A., Åström E.K.L., Hong W.-L., Portnov A., Waage M., Serov P., Carroll M. & Carroll J. 2018. Geophysical and geochemical controls on the megafaunal community of a High Arctic cold seep. *Biogeosciences 15*, 4533–4559, http://dx.doi.org/10.5194/bg-15-4533-2018.

Sen A., Himmler T., Hong W.-L., Chitkara C., Lee R.W., Ferré B., Lepland A. & Knies J. 2019. Atypical biological features of a new cold seep site on the Lofoten–Vesterålen continental margin (northern Norway). *Scientific Reports 9*, article no. 1762, http://dx.doi.org/10.1038/s41598-018-38070-9.

Shackleton N.J. 1974. Attainment of isotopic equilibrium between ocean water and the benthonic foraminifera genus *Uvigerina*: isotopic changes in the ocean during the last glacial. *Colloques Internationaux du C.N.R.S. 219*, 203–209.

Soltwedel T., Jaeckisch N., Ritter N., Hasemann C., Bergmann M. & Klages M. 2009. Bathymetric patterns of megafaunal assemblages from the Arctic deep-sea observatory Hausgarten. *Deep-Sea Research Part I 56*, 1856–1872, http://dx.doi.org/10.1016/j.dsr.2009.05.012.

Stuiver M. & Reimer P.J. 1993. Extended ^{14}C database and revised CALIB radiocarbon calibration program. *Radiocarbon 35*, 215–230.

Sztybor K. & Rasmussen T.L. 2017a. Diagenetic disturbances of marine sedimentary records from methane-influenced environments in the Fram Strait as indications of variation in seep intensity during the last 35000 years. *Boreas 46*, 212–228, http://dx.doi.org/10.1111/bor.12202.

Sztybor K. & Rasmussen T.L. 2017b. Late glacial and deglacial palaeoceanographic changes at Vestnesa Ridge, Fram Strait: methane seep versus non-seep environments. *Palaeogeography, Palaeoclimatology, Palaeoecology 476*, 77–89, http://dx.doi.org/10.1016/j.palaeo.2017.04.001.

Sztybor K., Rasmussen T.L., Mienert J., Bünz S. & Consolaro C. 2013. Climate reconstruction from a methane influenced environment. Abstract PP31A-1854. Poster presented at the AGU Fall Meeting. 9–13 December, San Francisco, CA.

Teichert B.M.A., Eisenhauer A., Bohrmann G., Haase-Schramm A., Bock B. & Linke P. 2003. U/Th systematics and ages of authigenic carbonates from Hydrate Ridge, Cascadia margIn: recorders of fluid flow variations. *Geochimica et Cosmochimica Acta 67*, 3845–3857, http://dx.doi.org/10.1016/S0016-7037(03)00128-5.

Thomsen E. 1987. *Environmental evaluation of pockmark areas near Gullfaks, Heimdal and Forties in the North Sea. Intern Skrift Serie 52*. Oslo: Institute of Geology, University of Oslo.

Thomsen E. & Vorren T.O. 1986. Macrofaunal palaeoecology and stratigraphy in Late Quaternary shelf sediments off northern Norway. *Palaeogeography, Palaeoclimatology, Palaeoecology 56*, 103–150, http://dx.doi.org/10.1016/0031-0182(86)90110-0.

Treude T., Boetius A., Knittel K., Wallmann K. & Jørgensen B.B. 2003. Anaerobic oxidation of methane above gas hydrates at Hydrate Ridge, NE Pacific Ocean. *Marine Ecology Progress Series 264*, 1–14, http://dx.doi.org/10.3354/meps264001.

Vinogradov G.M. 1999. Deep-sea near-bottom swarms of pelagic amphipods *Themisto*: observations from submersibles. *Sarsia 84*, 465–467, http://dx.doi.org/10.1080/00364827.1999.10807352.

Vogt P.R., Crane K., Sundvor E., Max M.D. & Pfirman S.L. 1994. Methane-generated (?) pockmarks on young, thickly sedimented oceanic crust in the Arctic: Vestnesa Ridge, Fram Strait. *Geology 22*, 255–258, http://dx.doi.org/10.1130/0091-7613(1994)022<0255:MGPOYT>2.3.CO;2.

Walczowski W., Piechura, J., Osinski, R. & Wieczorek, P. 2005. The West Spitsbergen Current volume and heat transport from synoptic observations in summer. *Deep Sea Research*

Part 1. Oceanographic Research Papers 52, 1374–1391, http://dx.doi.org/10.1016/j.dsr.2005.03.009.

Wallmann K., Riedel M., Hong W.L., Patton H., Hubbard A., Pape T., Hsu C.W., Schmidt C., Johnson J.E., Torres M.E., Andreassen K., Berndt C. & Bohrmann G. 2018. Gas hydrate dissociation off Svalbard induced by isostatic rebound rather than global warming. *Nature Communications 9*, article no. 83, http://dx.doi.org/10.1038/s41467-017-02550-9.

Wollenburg J.E., Kuhnt W. & Mackensen A. 2001. Changes in Arctic Ocean paleoproductivity and hydrography during the last 145 kyr: the benthic foraminiferal record. *Paleoceanography 16*, 65–77, http://dx.doi.org/0883-8305/01/1999PA00.